Supporting Information for

Radical Ions of 3-Styryl-quinoxalin-2-one Derivatives Studied by Pulse Radiolysis in Organic Solvents

Konrad Skotnicki,[1] Julio R. De la Fuente,[2] Álvaro Cañete,[3] Eduardo Berrios,[2] Krzysztof Bobrowski,[1,4*]*

[1] Institute of Nuclear Chemistry and Technology, 03-195 Warsaw, Poland

[2] Departamento de Química Orgánica y Fisicoquímica, Facultad de Ciencias Químicas y Farmacéuticas, Universidad de Chile, Casilla 223, Santiago 1, 6640750 Chile

[3] Departamento de Química Orgánica, Facultad de Química, Pontificia Universidad Católica de Chile, Casilla 306, Correo 22, Santiago, Chile

[4] Notre Dame Radiation Laboratory, University of Notre Dame, Notre Dame, IN 46556, USA

Contents:

Figure S1. Absorption spectra recorded in Ar- and O_2-saturated acetonitrile solutions containing 0.1 mM 3-(4-methylystyryl)quinoxalin-2(1*H*)-one (4-CH_3SQ). **P.S4**

Figure S2. Absorption spectra recorded in Ar- and O_2-saturated acetonitrile solutions containing 0.1 mM 3-(4-methoxystyryl)quinoxalin-2(1*H*)-one (4-OCH_3SQ). **P.S5**

Figure S3. Absorption spectra recorded in Ar- and O_2-saturated acetonitrile solutions containing 0.1 mM 3-(4-N,N-dimethylstyryl)quinoxalin-2(1*H*)-one (4-$N(CH_3)_2$ SQ). **P.S6**

Figure S4. Absorption spectra recorded in Ar- and O_2-saturated acetonitrile solutions containing 0.1 mM 3-(4-trifluoromethoxystyryl)quinoxalin-2(1*H*)-one (4-OCF_3SQ). **P.S7**

Figure S5. Absorption spectra recorded in Ar- and O_2-saturated acetonitrile solutions containing 0.1 mM 3-(3,4-dimethoxystyryl)quinoxalin-2(1*H*)-one (3,4-$(OCH_3)_2$SQ). **P.S8**

Figure S6. Absorption spectra recorded in Ar- and O_2-saturated acetonitrile solutions containing 0.1 mM 3-(2,5-dimethoxystyryl)quinoxalin-2(1*H*)-one (2,5-$(OCH_3)_2$SQ).

P.S9

Figure S7. Absorption spectra recorded in Ar-saturated 2-propanol solutions containing 0.1 mM 3-(4-methylystyryl)quinoxalin-2(1*H*)-one, (4-CH_3SQ) and absorption time profiles at selected wavelengths.

P.S10

Figure S8. Absorption spectra recorded in Ar-saturated 2-propanol solutions containing 0.1 mM 3-(4-methoxystyryl)quinoxalin-2(1*H*)-one, (4-OCH_3SQ) and absorption time profiles at selected wavelengths.

P.S11

Figure S9. Absorption spectra recorded in Ar-saturated 2-propanol solutions containing 0.1 mM 3-(4-N,N-dimethylstyryl)quinoxalin-2(1*H*)-one, (4-$N(CH_3)_2$SQ) and absorption time profiles at selected wavelengths.

P.S12

Figure S10. Absorption spectra recorded in Ar-saturated 2-propanol solutions containing 0.1 mM 3-(4-trifluoromethoxystyryl)quinoxalin-2(1*H*)-one, (4-OCF_3SQ) and absorption time profiles at selected wavelengths.

P.S13

Figure S11. Absorption spectra recorded in Ar-saturated 2-propanol solutions containing 0.1 mM 3-(3,4-dimethoxystyryl)quinoxalin-2(1*H*)-one, (3,4-$(OCH)_2$SQ) and absorption time profiles at selected wavelengths.

P.S14

Figure S12. Absorption spectra recorded in Ar-saturated 2-propanol solutions containing 0.1 mM 3-(2,5-dimethoxystyryl)quinoxalin-2(1*H*)-one, (2,5-$(OCH)_2$SQ) and absorption time profiles at selected wavelengths.

P.S15

Figure S13. Absorption spectra recorded in Ar-saturated acetonitrile solutions containing 0.1 mM 3-methylquinoxalin-2(1*H*)-one, (3-MeQ) and absorption time profiles at selected wavelengths.

P.S16

Figure S14. Absorption spectra recorded in O_2-saturated acetonitrile solutions containing 0.1 mM 3-methylquinoxalin-2(1*H*)-one, (3-MeQ) and absorption time profiles at selected wavelengths.

P.S17

Figure S15. Molecular orbitals involved in the electronic transitions for $SQ^{\bullet+}$, 4-$CH_3SQ^{\bullet+}$, 4-$OCF_3SQ^{\bullet+}$, and 4-$OCH_3SQ^{\bullet+}$.

P.S18

Figure S16. Molecular orbitals involved in the electronic transitions for 2,5-$(OCH_3)_2SQ^{\bullet+}$, 3,4-$(OCH_3)_2SQ^{\bullet+}$, 4-$N(CH_3)_2SQ^{\bullet+}$,

P.S19

Table S1. Formation enthalpies(ΔH_f) for the 3-$SQH^{\bullet}$ hydrogenated radicals.

P.S20

Table S2. M06-2x/def2-TZVP calculated vertical excitation energies treating acetonitrile implicitly.

P.S21

Table S3. M06-2x/def2-TZVP calculated vertical excitation energies treating acetonitrile implicitly.

P.S22

Table S4. CAM-B3LYP/def2-TZVP calculated vertical excitation energies in vacuum.

P.S23

The spectral characterization of **1a-1g** by ^1H NMR and HRMS-ESI (+ mode)

P.S24-P.S37

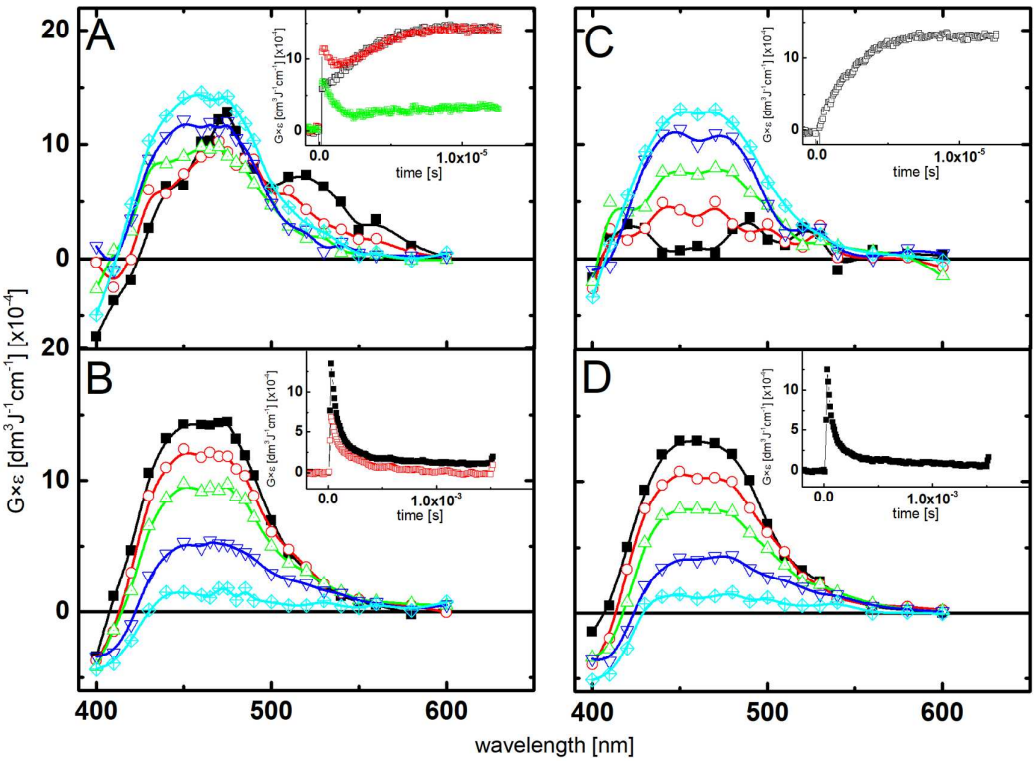

Figure S1. Absorption spectra recorded in Ar-saturated (A and B) acetonitrile solutions containing 0.1 mM 3-(4-methylystyryl)quinoxalin-2(1*H*)-one (4-CH_3SQ). Spectra taken after the following time delays: (A) 240 ns (■), 800 ns (○), 2 μs (△), 4 μs (▽), 8 μs (◊) and insert: short time profiles representing growth and/or decays at λ = 450 (□), 475 (○) and 520 nm (●); (B) 10μs (■), 24 μs (○), 40 μs (△), 100 μs (▽), 500 μs (◊) and insert: long-time profiles representing decays at λ = 450 (■), and 475 (□). Absorption spectra recorded in O_2-saturated (C and D) acetonitrile solutions containing 0.1 mM 3-(4-methylystyryl)quinoxalin-2(1*H*)-one, (4-CH_3SQ). Spectra taken after the following time delays: (C) 240 ns (■), 800 ns (○), 2 μs (△), 4 μs (▽), 8 μs (◊) and insert: short time profile representing growth at λ = 460 nm (□); (D) 10μs (■), 24 μs (○), 40 μs (△), 100 μs (▽), 500 μs (◊) and insert: long-time profile representing decay at λ = 460 nm (■).

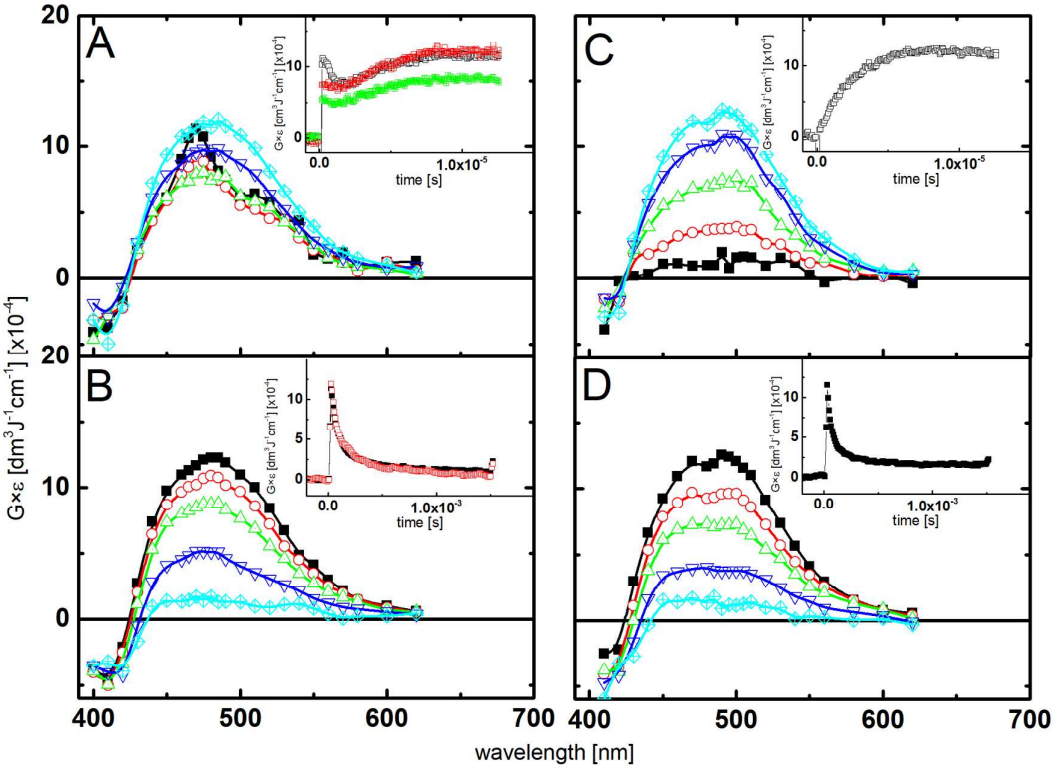

Figure S2. Absorption spectra recorded in Ar-saturated (A and B) acetonitrile solutions containing 0.1 mM 3-(4-methoxystyryl)quinoxalin-2(1*H*)-one (4-OCH_3SQ). Spectra taken after the following time delays: (A) 240 ns (■), 800 ns (○), 2 μs (△), 4 μs (▽), 8 μs (◊) and insert: short time profiles representing growth and/or decays at λ = 470 (□), 485 (○) and 510 nm (●); (B) 10μs (■), 24 μs (○), 40 μs (△), 100 μs (▽), 500 μs (◊) and insert: long-time profiles representing decays at λ = 470 (■), and 485 (□). Absorption spectra recorded in O_2-saturated (C and D) acetonitrile solutions containing 0.1 mM 3-(4-methoxystyryl)quinoxalin-2(1*H*)-one, (4-OCH_3SQ). Spectra taken after the following time delays: (C) 240 ns (■), 800 ns (○), 2 μs (△), 4 μs (▽), 8 μs (◊) and insert: short time profile representing growth at λ = 485 nm (□); (D) 10μs (■), 24 μs (○), 40 μs (△), 100 μs (▽), 500 μs (◊) and insert: long-time profile representing decay at λ = 485 nm (■).

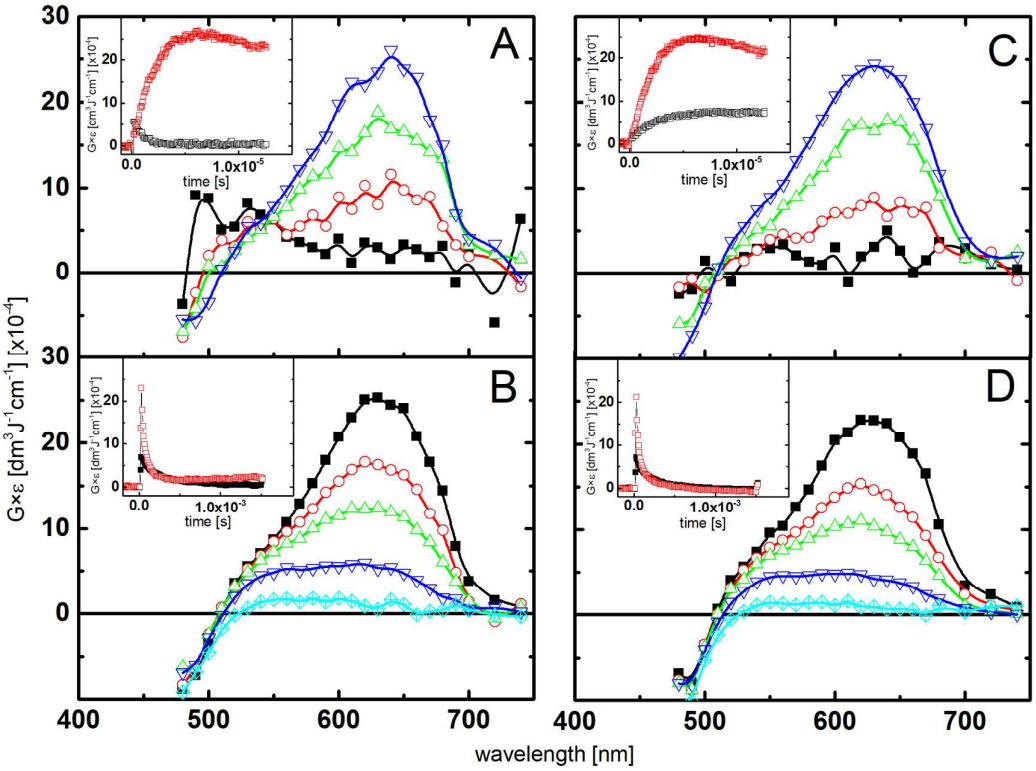

Figure S3. Absorption spectra recorded in Ar-saturated (A and B) acetonitrile solutions containing 0.1 mM 3-(4-*N*,*N*-dimethylstyryl)quinoxalin-2(1*H*)-one (4-Me$_2$NSQ). Spectra taken after the following time delays: (A) 240 ns (■), 800 ns (○), 2 μs (△), 4 μs (▽) and insert: short time profiles representing growth and/or decays at λ = 500 (□) and 630 (○); (B) 10μs (■), 24 μs (○), 40 μs (△), 100 μs (▽), 500 μs (◊) and insert: long-time profiles representing decays at λ = 500 (■) and 630 (□). Absorption spectra recorded in O_2-saturated (C and D) acetonitrile solutions containing 0.1 mM 3-(4-*N*,*N*-dimethylstyryl)quinoxalin-2 (1*H*)-one, (4-Me$_2$NSQ). Spectra taken after the following time delays: (C) 240 ns (■), 800 ns (○), 2 μs (△), 4 μs (▽) and insert: short time profile representing growth at λ = 630 nm (□) and 540 nm (○); (D) 10μs (■), 24 μs (○), 40 μs (△), 100 μs (▽), 500 μs (◊) and insert: long-time profile representing decay at λ = 630 nm (□) and 540 nm (○).

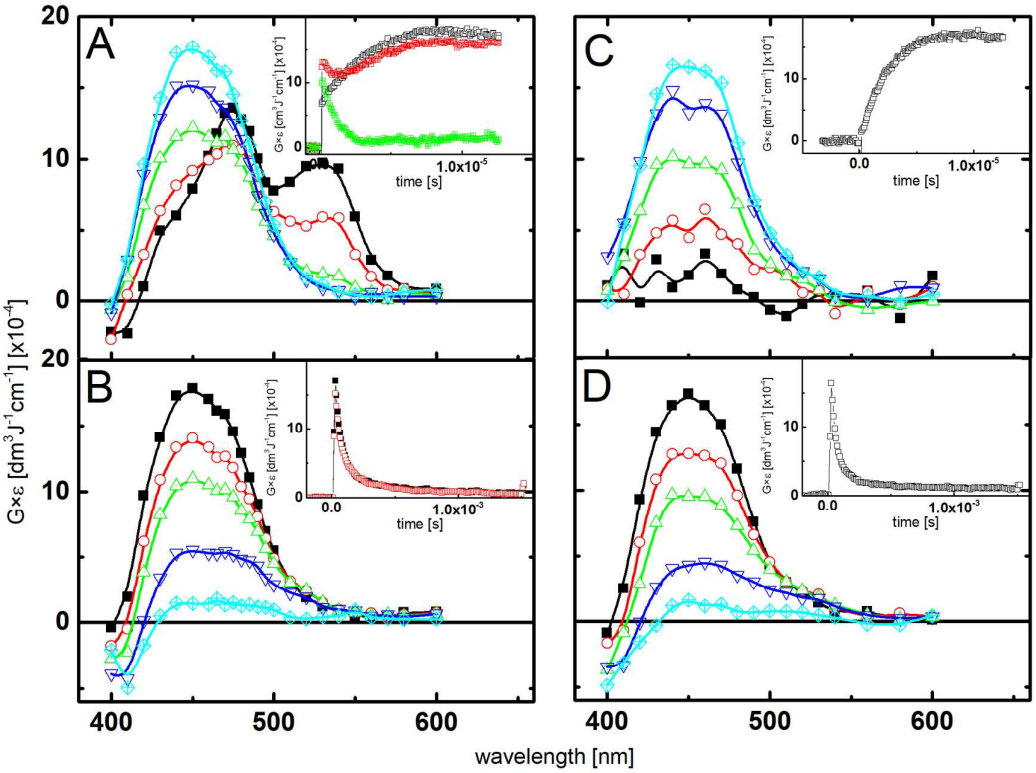

Figure S4. Absorption spectra recorded in Ar-saturated (A and B) acetonitrile solutions containing 0.1 mM 3-(4-trifluoromethoxystyryl)quinoxalin-2(1*H*)-one (4-OCF_3SQ). Spectra taken after the following time delays: (A) 240 ns (■), 800 ns (○), 2 μs (△), 4 μs (▽), 8 μs (◊) and insert: short time profiles representing growth and/or decays at λ = 450 (□), 475 (○) and 530 nm (●); (B) 10μs (■), 24 μs (○), 40 μs (△), 100 μs (▽), 500 μs (◊) and insert: long-time profiles representing decays at λ = 450 (■), and 475 (□). Absorption spectra recorded in O_2-saturated (C and D) acetonitrile solutions containing 0.1 mM 3-(4-trifluoromethoxystyryl)quinoxalin-2(1*H*)-one, (4-OCF_3SQ). Spectra taken after the following time delays: (C) 240 ns (■), 800 ns (○), 2 μs (△), 4 μs (▽), 8 μs (◊) and insert: short time profile representing growth at λ = 450 nm (□); (D) 10μs (■), 24 μs (○), 40 μs (△), 100 μs (▽), 500 μs (◊) and insert: long-time profile representing decay at λ = 450 nm (■).

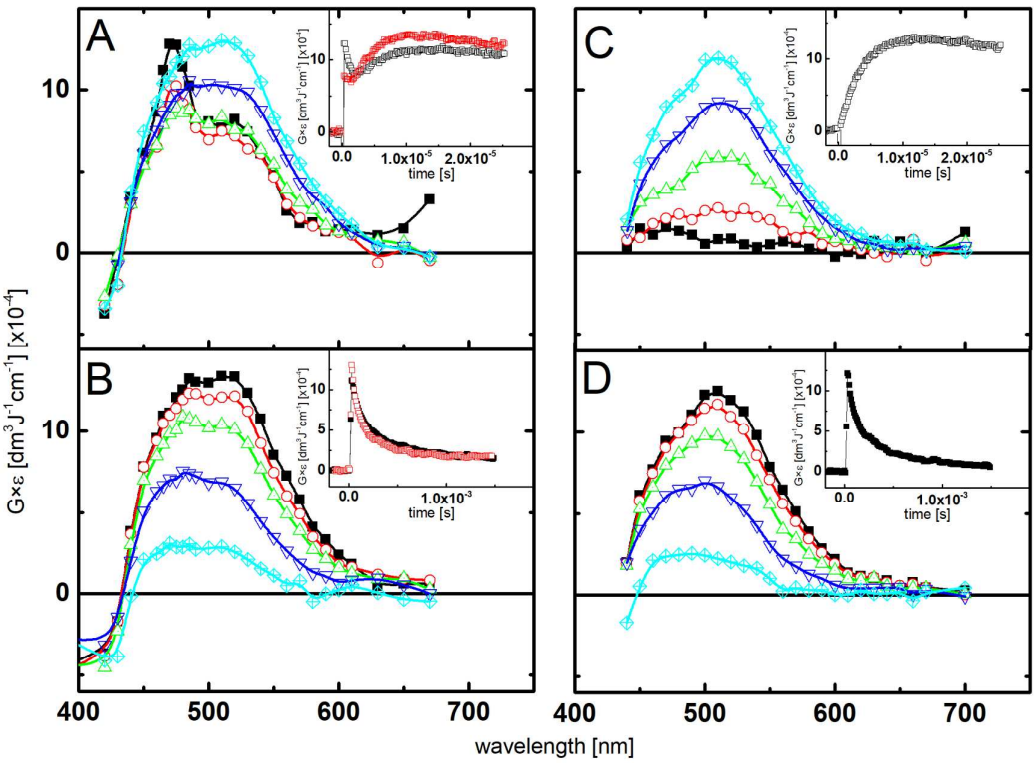

Figure S5. Absorption spectra recorded in Ar-saturated (A and B) acetonitrile solutions containing 0.1 mM 3-(3,4-dimethoxystyryl)quinoxalin-2(1*H*)-one, (3,4-(OCH)$_2$SQ). Spectra taken after the following time delays: (A) 240 ns (■), 800 ns (○), 2 μs (△), 4 μs (▽), 8 μs (◊) and insert: short time profiles representing growth and/or decays at λ = 470 (□) and 510 nm (○); (B) 10μs (■), 24 μs (○), 40 μs (△), 100 μs (▽), 500 μs (◊) and insert: long-time profiles representing decays at λ = 470 (■), and 510 (□). Absorption spectra recorded in O_2-saturated (C and D) acetonitrile solutions containing 0.1 mM 3-(3,4-dimethoxystyryl)quinoxalin-2 (1*H*)-one, (3,4-(OCH)$_2$SQ). Spectra taken after the following time delays: (C) 240 ns (■), 800 ns (○), 2 μs (△), 4 μs (▽), 8 μs (◊) and insert: short time profile representing growth at λ = 520 nm (□); (D) 10μs (■), 24 μs (○), 40 μs (△), 100 μs (▽), 500 μs (◊) and insert: long-time profile representing decay at λ = 510 nm (■).

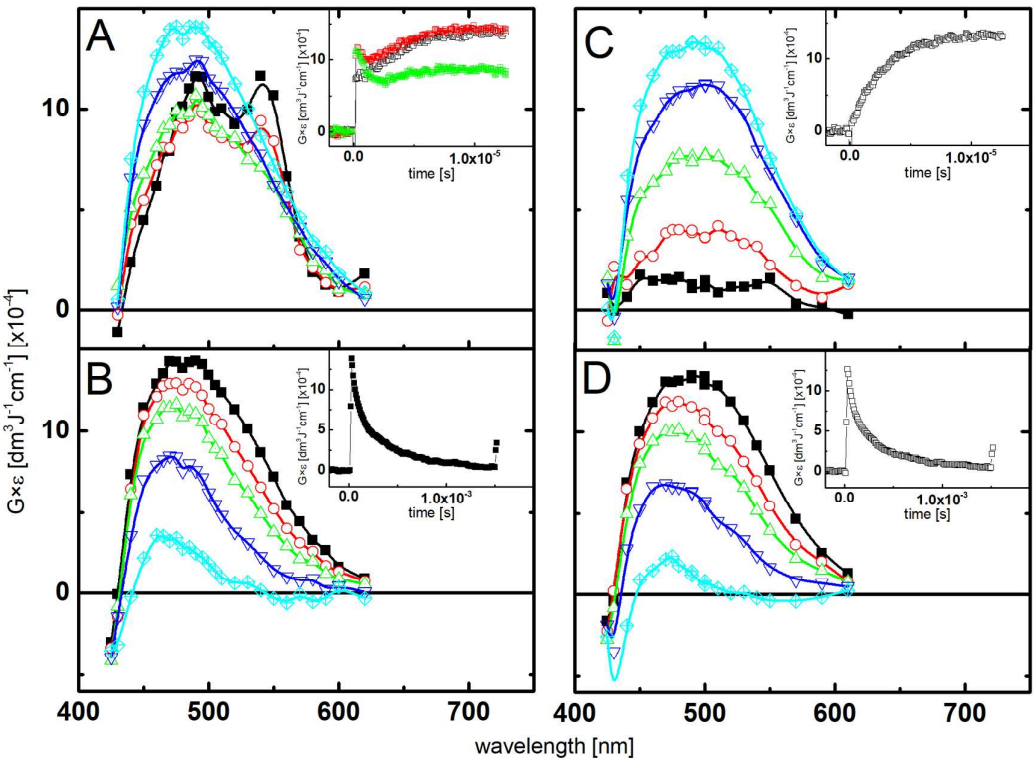

Figure S6 Absorption spectra recorded in Ar-saturated (A and B) acetonitrile solutions containing 0.1 mM 3-(2,5-dimethoxystyryl)quinoxalin-2(1*H*)-one (2,5-$(OCH)_2$SQ). Spectra taken after the following time delays: (A) 240 ns (■), 800 ns (○), 2 μs (△), 4 μs (▽), 8 μs (◊) and insert: short time profiles representing growth and/or decays at λ = 470 (□) and 520 nm (○); (B) 10μs (■), 24 μs (○), 40 μs (△), 100 μs (▽), 500 μs (◊) and insert: long-time profiles representing decays at λ = 470 (■), and 520 (□). Absorption spectra recorded in O_2-saturated (C and D) acetonitrile solutions containing 0.1 mM 3-(2,5-dimethoxystyryl)quinoxalin-2 (1*H*)-one, (2,5-$(OCH)_2$SQ). Spectra taken after the following time delays: (C) 240 ns (■), 800 ns (○), 2 μs (△), 4 μs (▽), 8 μs (◊) and insert: short time profile representing growth at λ = 510 nm (□); (D) 10μs (■), 24 μs (○), 40 μs (△), 100 μs (▽), 500 μs (◊) and insert: long-time profile representing decay at λ = 510 nm (■).

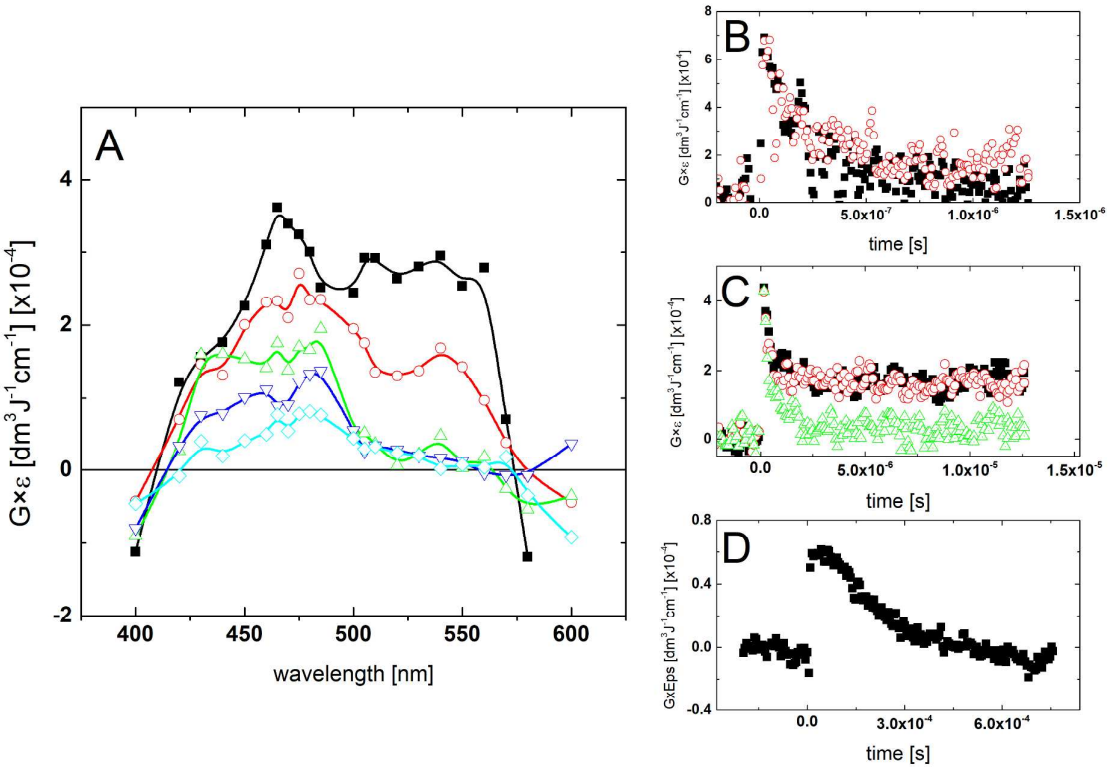

Figure S7. Absorption spectra recorded in Ar-saturated 2-propanol solutions containing 0.1 mM 3-(4-methylystyryl)quinoxalin-2(1*H*)-one, (4-CH_3SQ). Spectra taken after the following time delays: 240 ns (■), 480 ns (○), 1 μs (△), 10 μs (▽), 100 μs (◇) **(A)**; short time profiles representing decays at λ = 460 (■), and 520 nm (○) (**B**); short time profiles representing decays at λ = 450 (■), 480 (○), and 520 nm (△) **(C);** a long-time profile representing decay at λ = 480 nm (■) (**D**).

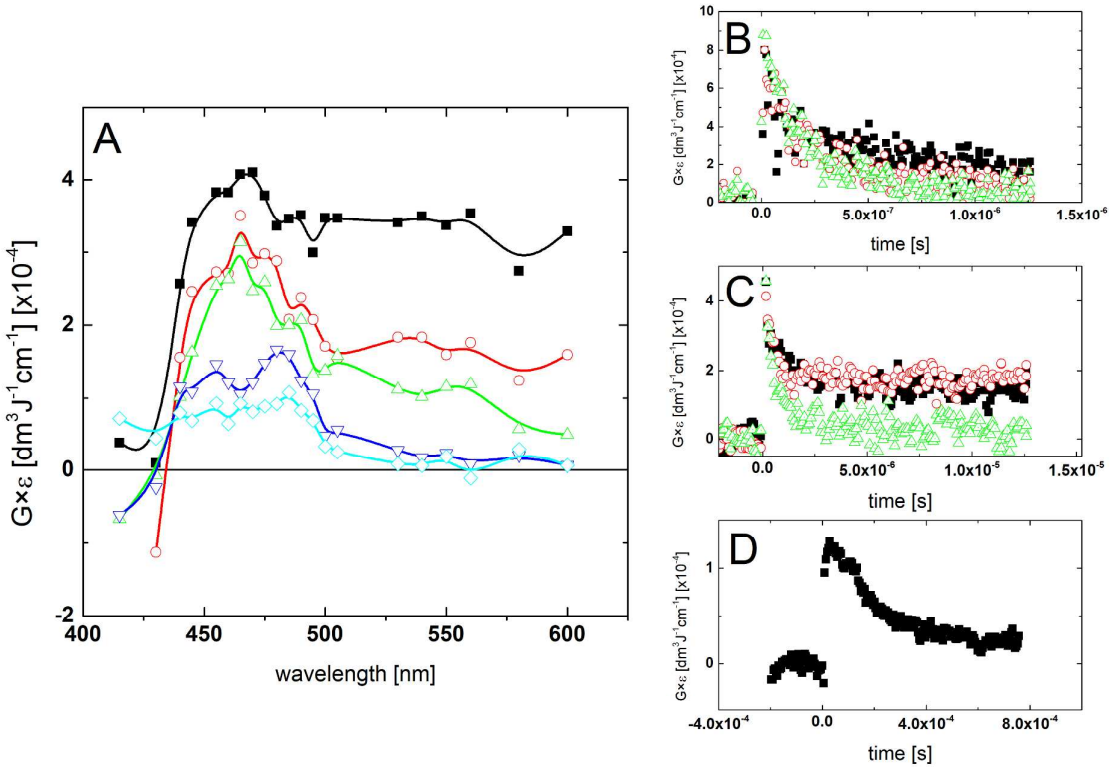

Figure S8. Absorption spectra recorded in Ar-saturated 2-propanol solutions containing 0.1 mM 3-(4-methoxystyryl)quinoxalin-2(1*H*)-one, (4-OCH_3SQ). Spectra taken after the following time delays: 240 ns (■), 480 ns (○), 1 μs (△), 10 μs (▽), 100 μs (◊) **(A)**; short time profiles representing decays at λ = 470 (■), 540 (○) and 600 nm (△) (**B**); short time profiles representing decays at λ = 450 (■), 480 (○), and 540 nm (△) **(C);** a long-time profile representing decay at λ = 480 nm (■) (**D**).

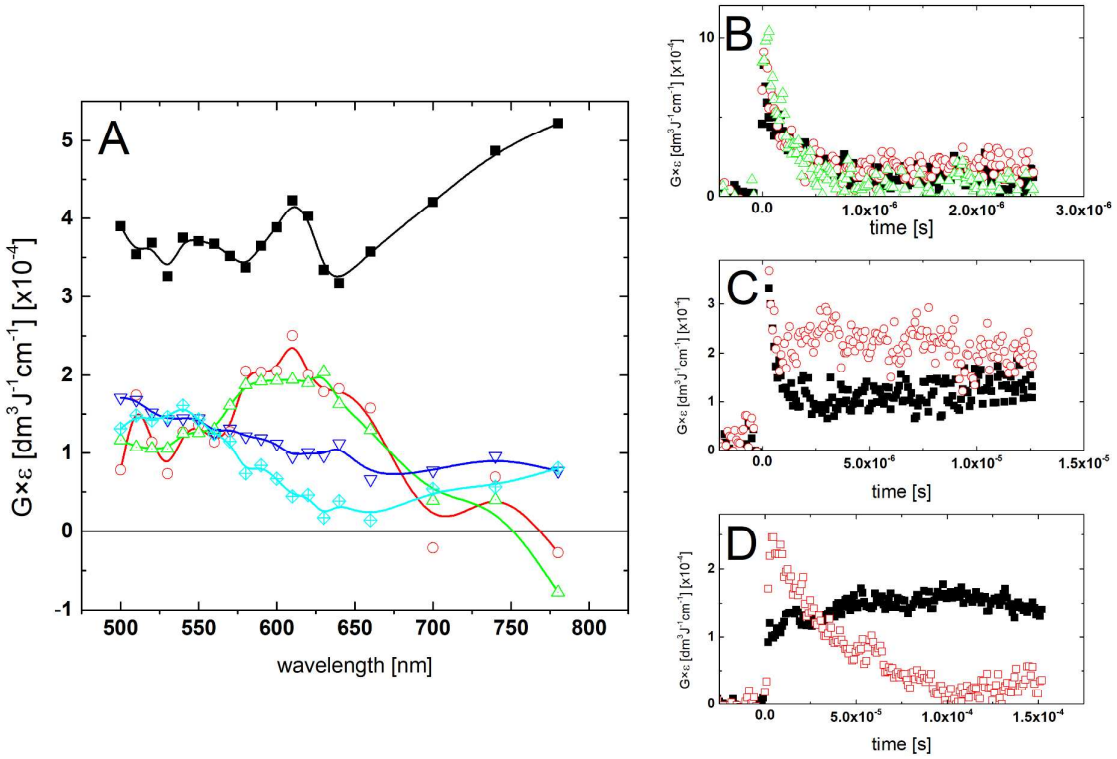

Figure S9. Absorption spectra recorded in Ar-saturated 2-propanol solutions containing 0.1 mM 3-(4-N,N-dimethylstyryl)quinoxalin-2(1*H*)-one, (4-N(CH_3)$_2$SQ). Spectra taken after the following time delays: 240 ns (■), 1 μs (○), 10 μs (△), 40 μs (▽) and 100 μs (◇) **(A)**; short time profiles representing decays at λ = 540 (■), 630 (○) and 700 nm (△) (**B**); short time profiles representing decays at λ = 540 (■) and 630 nm (○); **(C);** a long-time profile representing growth and decay at λ = 540 (■) and 630 nm (○).

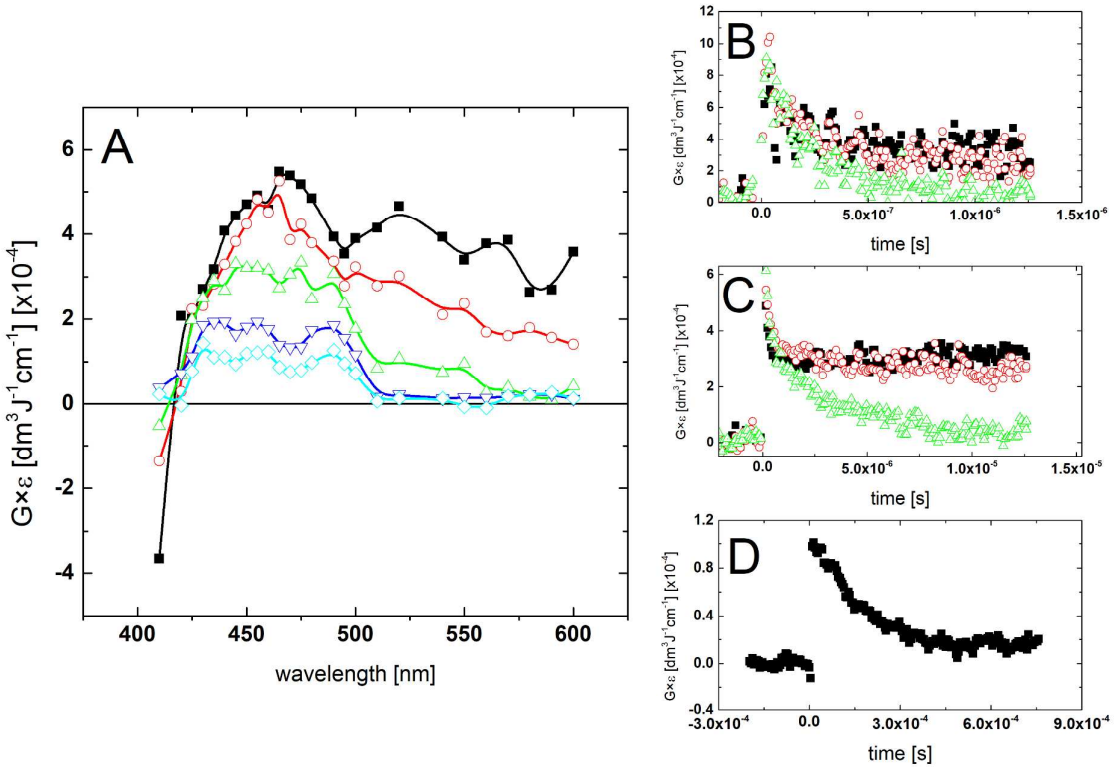

Figure S10. Absorption spectra recorded in Ar-saturated 2-propanol solutions containing 0.1 mM 3-(4-trifluoromethoxystyryl)quinoxalin-2(1*H*)-one (4-OCF_3SQ). Spectra taken after the following time delays: 240 ns (■), 480 ns (○), 1 μs (△), 10 μs (▽), 100 μs (◊) **(A)**; short time profiles representing decays at λ = 470 (■), 520 (○) and 600 nm (△) (**B**); short time profiles representing decays at λ = 430 (■), 490 (○), and 520 nm (△) **(C);** a long-time profile representing decay at λ = 490 nm (■) (**D**).

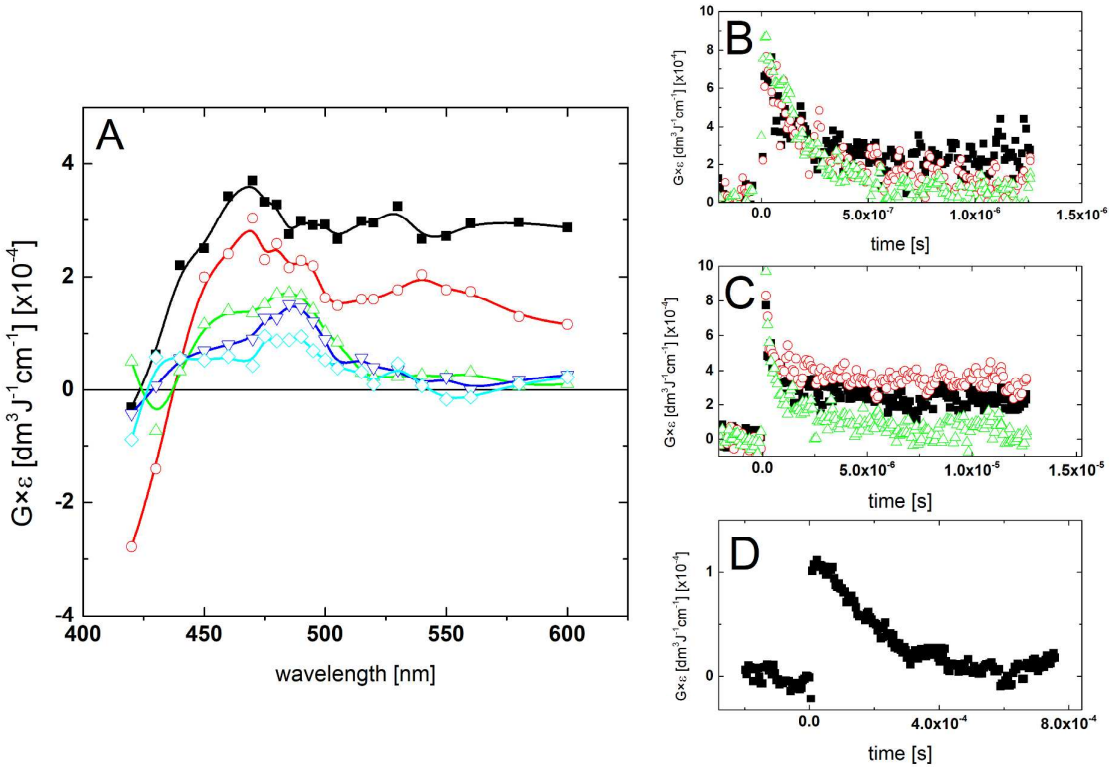

Figure S11. Absorption spectra recorded in Ar-saturated 2-propanol solutions containing 0.1 mM 3-(3,4-dimethoxystyryl)quinoxalin-2(1*H*)-one, (3,4-$(OCH)_2$SQ). Spectra taken after the following time delays: 240 ns (■), 480 ns (○), 1 μs (△), 10 μs (▽), 100 μs (◊) **(A)**; short time profiles representing decays at λ = 470 (■), 520 (○) and 600 nm (△) (**B**); short time profiles representing decays at λ = 450 (■), 480 (○), and 530 nm (△) **(C);** a long-time profile representing decay at λ = 480 nm (■) (**D**).

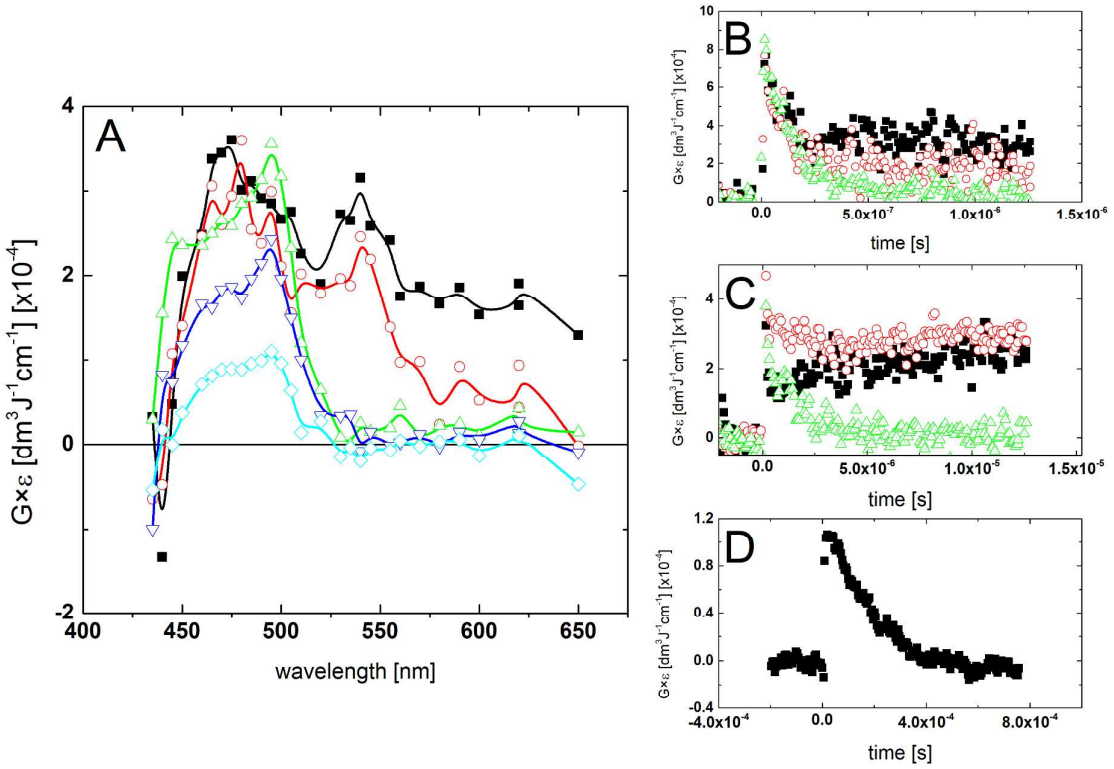

Figure S12. Absorption spectra recorded in Ar-saturated 2-propanol solutions containing 0.1 mM 3-(2,5-dimethoxystyryl)quinoxalin-2(1*H*)-one, (2,5-(OCH)$_2$SQ). Spectra taken after the following time delays: 240 ns (■), 480 ns (○), 1 μs (△), 10 μs (▽), 100 μs (◊) **(A)**; short time profiles representing decays at λ = 475 (■), 540 (○) and 600 nm (△) (**B**); short time profiles representing decays at λ = 450 (■), 490 (○), and 540 nm (△) **(C);** a long-time profile representing decay at λ = 490 nm (■) (**D**).

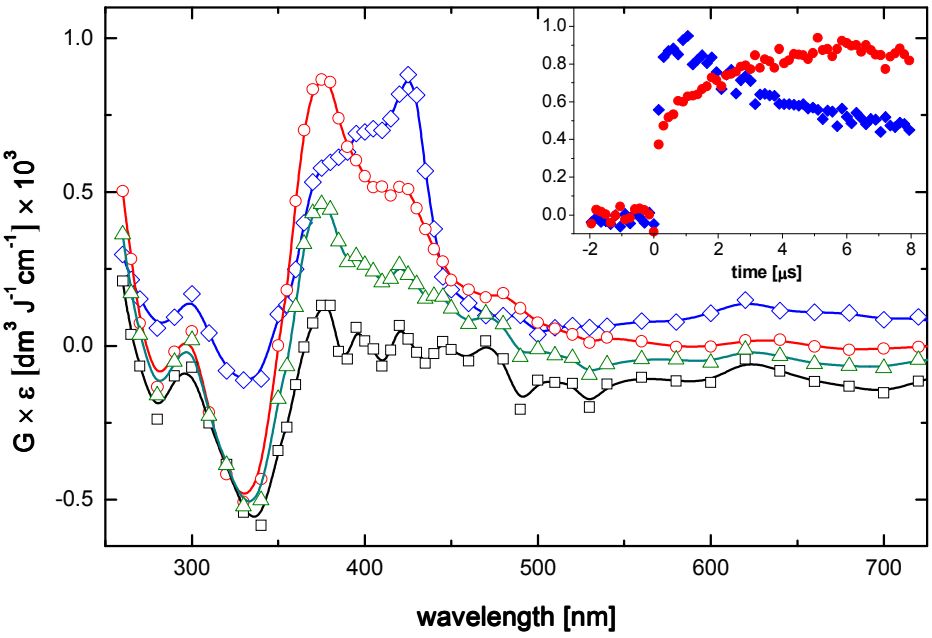

Figure S13. Absorption spectra recorded in Ar-saturated acetonitrile solutions containing 0.1 mM 3-methyl—1*H*-quinoxalin-2(1*H*)-one, (3-MeQ). Spectra taken after the following time delays: 600 ns (◇), 6 µs (○), 25 µs (△), 50 µs (□): inset: short-time profiles representing formation at λ = 375 nm (●)and formation and decay at λ = 425 nm (◆).

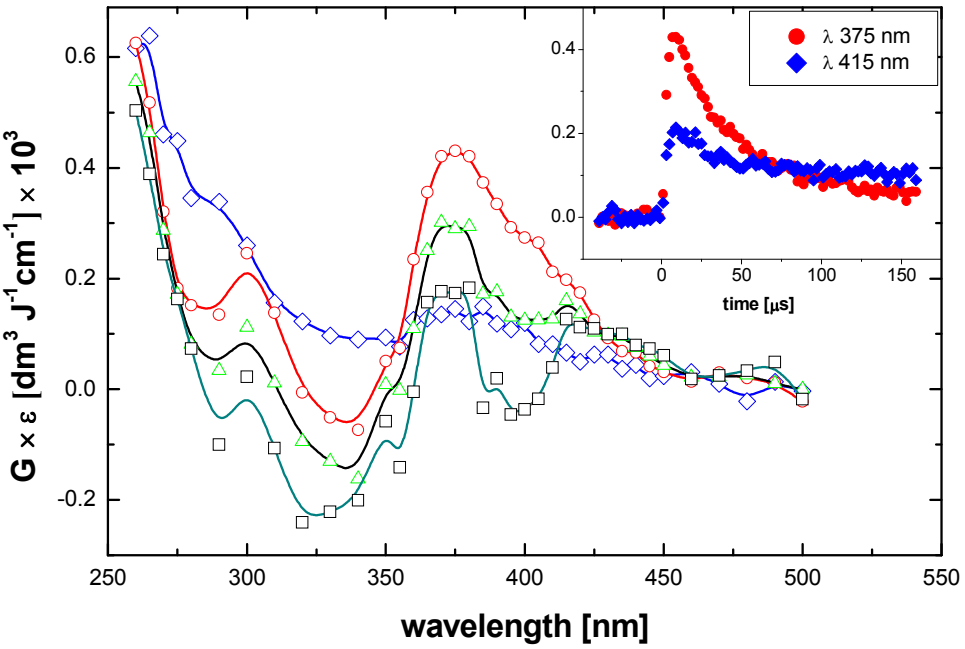

Figure S14. Absorption spectra recorded in O_2-saturated acetonitrile solutions containing 0.1 mM 3-methyl—1*H*-quinoxalin-2(1*H*)-one, (3-MeQ). Spectra taken after the following time delays: 600 ns (◇), 6 μs (○), 25 μs (△), 50 μs (□): inset: long-time profiles representing decays at λ = 375 nm (●) and λ = 425 nm (◆).

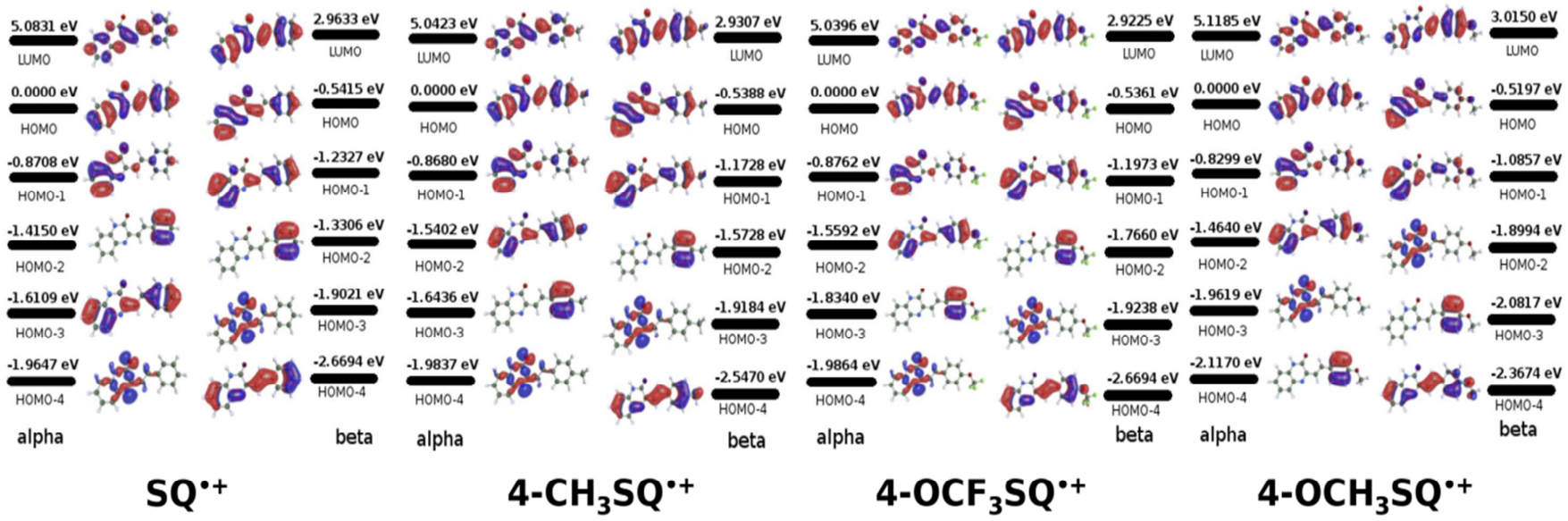
5.0831 eV
LUMO
0.0000 eV
HOMO
-0.8708 eV
HOMO-1
-1.4150 eV
HOMO-2
-1.6109 eV
HOMO-3
-1.9647 eV
HOMO-4
alpha
2.9633 eV
LUMO
-0.5415 eV
HOMO
-1.2327 eV
HOMO-1
-1.3306 eV
HOMO-2
-1.9021 eV
HOMO-3
-2.6694 eV
HOMO-4
beta
SQ•+
5.0423 eV
LUMO
0.0000 eV
HOMO
-0.8680 eV
HOMO-1
-1.5402 eV
HOMO-2
-1.6436 eV
HOMO-3
-1.9837 eV
HOMO-4
alpha
2.9307 eV
LUMO
-0.5388 eV
HOMO
-1.1728 eV
HOMO-1
-1.5728 eV
HOMO-2
-1.9184 eV
HOMO-3
-2.5470 eV
HOMO-4
beta
4-CH3SQ•+
5.0396 eV
LUMO
0.0000 eV
HOMO
-0.8762 eV
HOMO-1
-1.5592 eV
HOMO-2
-1.8340 eV
HOMO-3
-1.9864 eV
HOMO-4
alpha
2.9225 eV
LUMO
-0.5361 eV
HOMO
-1.1973 eV
HOMO-1
-1.7660 eV
HOMO-2
-1.9238 eV
HOMO-3
-2.6694 eV
HOMO-4
beta
4-OCF3SQ•+
5.1185 eV
LUMO
0.0000 eV
HOMO
-0.8299 eV
HOMO-1
-1.4640 eV
HOMO-2
-1.9619 eV
HOMO-3
-2.1170 eV
HOMO-4
alpha
3.0150 eV
LUMO
-0.5197 eV
HOMO
-1.0857 eV
HOMO-1
-1.8994 eV
HOMO-2
-2.0817 eV
HOMO-3
-2.3674 eV
HOMO-4
beta
4-OCH3SQ•+

Figure S15.

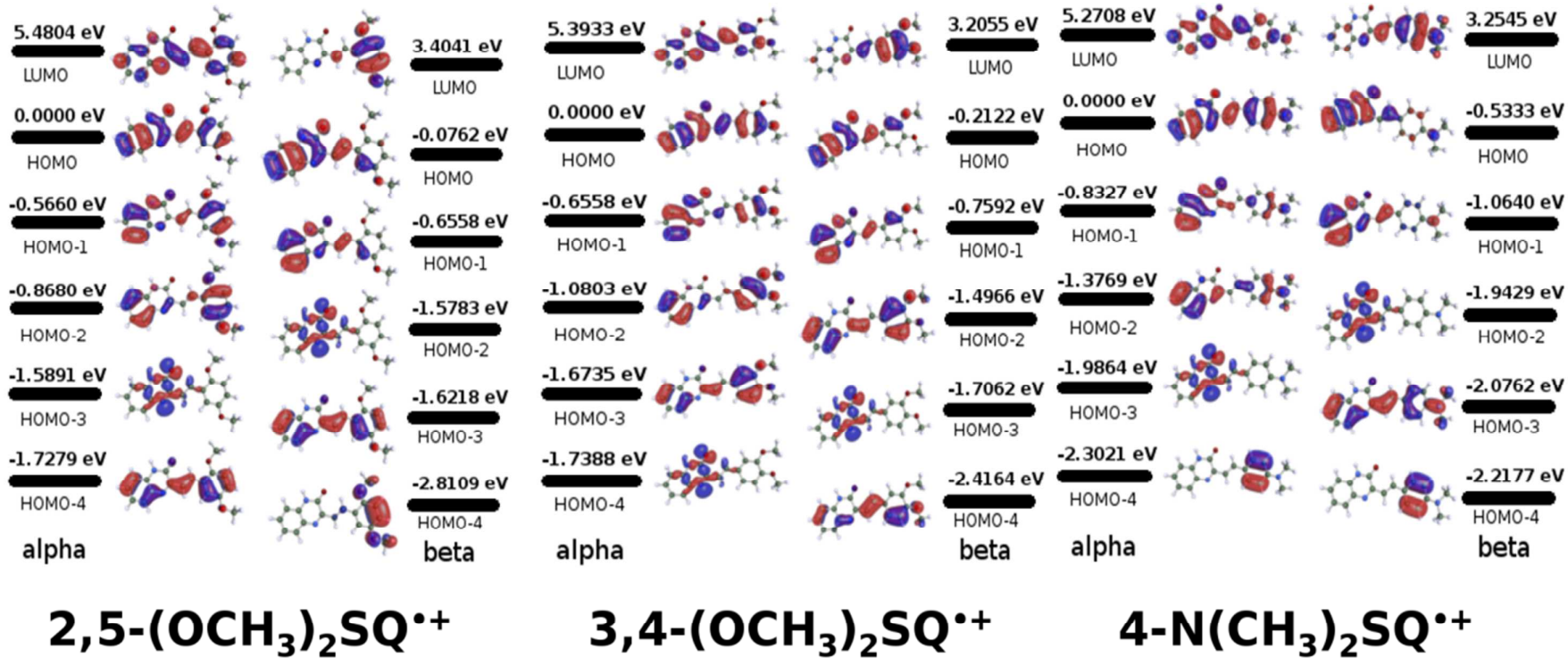
5.4804 eV
LUMO
0.0000 eV
HOMO
-0.5660 eV
HOMO-1
-0.8680 eV
HOMO-2
-1.5891 eV
HOMO-3
-1.7279 eV
HOMO-4
alpha
3.4041 eV
LUMO
-0.0762 eV
HOMO
-0.6558 eV
HOMO-1
-1.5783 eV
HOMO-2
-1.6218 eV
HOMO-3
-2.8109 eV
HOMO-4
beta
2,5-(OCH3)2SQ•+
5.3933 eV
LUMO
0.0000 eV
HOMO
-0.6558 eV
HOMO-1
-1.0803 eV
HOMO-2
-1.6735 eV
HOMO-3
-1.7388 eV
HOMO-4
alpha
3.2055 eV
LUMO
-0.2122 eV
HOMO
-0.7592 eV
HOMO-1
-1.4966 eV
HOMO-2
-1.7062 eV
HOMO-3
-2.4164 eV
HOMO-4
beta
3,4-(OCH3)2SQ•+
5.2708 eV
LUMO
0.0000 eV
HOMO
-0.8327 eV
HOMO-1
-1.3769 eV
HOMO-2
-1.9864 eV
HOMO-3
-2.3021 eV
HOMO-4
alpha
3.2545 eV
LUMO
-0.5333 eV
HOMO
-1.0640 eV
HOMO-1
-1.9429 eV
HOMO-2
-2.0762 eV
HOMO-3
-2.2177 eV
HOMO-4
beta
4-N(CH3)2SQ•+

Figure S16.

Table S1: Formation enthalpies (ΔH_f) for the 3-SQH$^{\bullet}$ hydrogenated radicals.

Compound	Ground State	Rad SQNH$^{\bullet}$[a]	Rad SQOH$^{\bullet}$	Rad CH11SQ$^{\bullet}$	Rad CH12SQ$^{\bullet}$
		ΔH_f kcal mol^{-1}			
3-SQ	44.890	31.997	42.604	38.352	37.640
4-CH_3SQ	35.198	22.397	32.743	28.038	28.519
4-OCH_3SQ	6.393	-6.326	4.112	-0.207	-1.840
4-$N(CH_3)_2$SQ	40.825	27.924	38.360	35.407	35.038
4-OCF_3SQ	-158.558	-171.629	-160.940	-165.305	-166.551
3,4-$(OCH_3)_2$SQ	-28.017	-41.283	-30.740	-34.863	-33.808
2,5-$(OCH_3)_2$SQ	-27.650	-41.260	-31.340	-35.448	-35.599

[a] for all compounds the most stable radicals are those hydrogenated over N4.

Table S2. M06-2x/def2-TZVP calculated vertical excitation energies treating acetonitrile implicitly.

M06-2x/def2-TZVP COSMO												
	$SQ^{\bullet+}$			4-$CH_3SQ^{\bullet+}$			4-$OCF_3SQ^{\bullet+}$			4-$OCH_3SQ^{\bullet+}$		
	λ / nm	f[a]	w / %[b]	λ / nm	f[a]	w / %[b]	λ / nm	f[a]	w / %[b]	λ / nm	f[a]	w / %[b]
S1	980	0.159	$H_\beta \rightarrow L_\beta$ (94)	925	0.257	$H_\beta \rightarrow L_\beta$ (94)	969	0.208	$H_\beta \rightarrow L_\beta$ (94)	801	0.354	$H_\beta \rightarrow L_\beta$ (87)
S2	655	0.207	H-$1_\beta \rightarrow L_\beta$ (86)	651	0.162	H-$1_\beta \rightarrow L_\beta$ (87)	663	0.210	H-$1_\beta \rightarrow L_\beta$ (87)	589	0.053	H-$1_\beta \rightarrow L_\beta$ (75)
S3	630	0.000[c]	H-$3_\beta \rightarrow L_\beta$ (92)	598	0.004	H-$2_\beta \rightarrow L_\beta$ (85)	619	0.000[c]	H-$3_\beta \rightarrow L_\beta$ (91)	528	0.000[c]	H-$2_\beta \rightarrow L_\beta$ (83)
S4	596	0.003	H-$2_\beta \rightarrow L_\beta$ (91)	597	0.000[c]	H-$3_\beta \rightarrow L_\beta$ (83)	518	0.003	H-$2_\beta \rightarrow L_\beta$ (91)	527	0.002	H-$3_\beta \rightarrow L_\beta$ (90)
S5	452	0.867	$H_\alpha \rightarrow L_\alpha$ (85)	457	0.934	$H_\alpha \rightarrow L_\alpha$ (84)	457	0.93	$H_\alpha \rightarrow L_\alpha$ (85)	450	0.865	$H_\alpha \rightarrow L_\alpha$ (73)
S6	404	0.025	H-$4_\beta \rightarrow L_\beta$ (60)	422	0.025	H-$4_\beta \rightarrow L_\beta$ (64)	413	0.022	H-$4_\beta \rightarrow L_\beta$ (63)	431	0.08	H-$4_\beta \rightarrow L_\beta$ (61)
S7	383	0.000	H-$5_\beta \rightarrow L_\beta$ (68)	372	0.114	H-$1_\alpha \rightarrow L_\alpha$ (37)	378	0.000	H-$5_\beta \rightarrow L_\beta$ (68)	363	0.203	H-$1_\alpha \rightarrow L_\alpha$ (38)
S8	372	0.066	H-$1_\alpha \rightarrow L_\alpha$ (39)	371	0.002	H-$5_\beta \rightarrow L_\beta$ (62)	374	0.08	H-$1_\alpha \rightarrow L_\alpha$ (38)	344	0.000	H-$5_\beta \rightarrow L_\beta$ (46)
$\langle S^2 \rangle$	0.785(4.7%)			0.787(4.9%)			0.785(4.7%)			0.792(5.6%)		

[a] oscillator strengths for each transition; [b] main molecular orbital contribution for each transition; [c] all transitions with oscillator strengths smaller than 0.001 were assigned as 0

Table S3. M06-2x/def2-TZVP calculated vertical excitation energies treating acetonitrile implicitly.

M06-2x/def2-TZVP COSMO									
	$2,5(OCH_3)_2SQ^{\bullet+}$			$3,4(OCH_3)_2SQ^{\bullet+}$			$4N(CH_3)_2SQ^{\bullet+}$		
	λ / nm	f[a]	w / %[b]	λ / nm	f[a]	w / %[b]	λ / nm	f[a]	w / %[b]
S1	876	0.086	$H_\beta \rightarrow L_\beta$ (60)	972	0.173	$H_\beta \rightarrow L_\beta$ (54)	679	0.339	$H_\beta \rightarrow L_\beta$ (65)
S2	499	0.002	$H_\beta \rightarrow L{+}1_\beta$ (19) $H_\alpha \rightarrow L_\alpha$ (19)	598	0.128	$H\text{-}2_\beta \rightarrow L_\beta$ (37) $H_\beta \rightarrow L_\beta$ (30)	484	0.001	$H\text{-}4_\beta \rightarrow L_\beta$ (65)
S3	461	0.073	$H_\alpha \rightarrow L_\alpha$ (27) $H\text{-}1_\beta \rightarrow L_\beta$ (25)	489	0.005	$H\text{-}1_\beta \rightarrow L_\beta$ (53)	481	0.002	$H\text{-}1_\beta \rightarrow L_\beta$ (35) $H\text{-}4_\beta \rightarrow L_\beta$ (29)
S4	408	0.140	$H\text{-}4_\beta \rightarrow L_\beta$ (51)	444	0.458	$H_\alpha \rightarrow L_\alpha$ (52)	440	0.67	$H_\alpha \rightarrow L_\alpha$ (56)
S5	388	0.000[c]	$H\text{-}2_\beta \rightarrow L_\beta$ (68)	431	0.000[c]	$H\text{-}3_\beta \rightarrow L_\beta$ (76)	422	0.000	$H\text{-}2_\beta \rightarrow L_\beta$ (70)
S6	377	0.081	$H\text{-}3_\beta \rightarrow L_\beta$ (29) $H\text{-}4_\beta \rightarrow L_\beta$ (26)	384	0.07	$H\text{-}4_\beta \rightarrow L_\beta$ (38) $H\text{-}2_\beta \rightarrow L_\beta$ (21)	393	0.31	$H\text{-}3_\beta \rightarrow L_\beta$ (37) $H\text{-}1_\beta \rightarrow L_\beta$ (21)
S7	361	0.117	$H\text{-}1_\alpha \rightarrow L_\alpha$ (33) $H\text{-}1_\beta \rightarrow L_\beta$ (14)	356	0.216	$H\text{-}1_\alpha \rightarrow L_\alpha$ (38) $H_\beta \rightarrow L{+}1_\beta$ (11)	350	0.24	$H\text{-}1_\alpha \rightarrow L_\alpha$ (35) $H_\beta \rightarrow L{+}1_\beta$ (15)
S8	340	0.596	$H_\beta \rightarrow L{+}1_\beta$ (41) $H_\alpha \rightarrow L_\alpha$ (34)	335	0.004	$H\text{-}7_\beta \rightarrow L_\beta$ (60)	318	0.000[c]	$H\text{-}3_\alpha \rightarrow L_\alpha$ (59)
$\langle S^2 \rangle$	0.766(2.1%)			0.778(3.7%)			0.799(6.5%)		

[a] oscillator strengths for each transition; [b] main molecular orbital contribution for each transition; [c] all transitions with oscillator strengths smaller than 0.001 were assigned as 0

Table S4. CAM-B3LYP/def2-TZVP calculated vertical excitation energies in vacuum.

CAM-B3LYP/def2-TZVP									
	$2,5(OCH_3)_2SQ^{\bullet+}$			$3,4(OCH_3)_2SQ^{\bullet+}$			$4N(CH_3)_2SQ^{\bullet+}$		
	λ / nm	f[a]	w / %[b]	λ / nm	f[a]	w / %[b]	λ / nm	f[a]	w / %[b]
S1	1339	0.149	$H_\beta \rightarrow L_\beta$ (69)	889	0.314	$H_\beta \rightarrow L_\beta$ (84)	796	0.361	$H_\beta \rightarrow L_\beta$ (72)
S2	686	0.023	$H\text{-}1_\beta \rightarrow L_\beta$ (49)	675	0.002	$H\text{-}1_\beta \rightarrow L_\beta$ (59)	586	0.002	$H\text{-}1_\beta \rightarrow L_\beta$ (53)
S3	604	0.063	$H_\alpha \rightarrow L_\alpha$ (37) $H\text{-}3_\beta \rightarrow L_\beta$ (10)	616	0.000[c]	$H\text{-}2_\beta \rightarrow L_\beta$ (82)	556	0.000[c]	$H\text{-}2_\beta \rightarrow L_\beta$ (76)
S4	584	0.000[c]	$H\text{-}2_\beta \rightarrow L_\beta$ (84)	589	0.002	$H\text{-}3_\beta \rightarrow L_\beta$ (54)	513	0.548	$H_\alpha \rightarrow L_\alpha$ (43)
S5	494	0.294	$H\text{-}3_\beta \rightarrow L_\beta$ (43)	502	0.787	$H_\alpha \rightarrow L_\alpha$ (55)	472	0.003	$H\text{-}4_\beta \rightarrow L_\beta$ (88)
S6	422	0.027	$H\text{-}6_\beta \rightarrow L_\beta$ (31) $H\text{-}4_\alpha \rightarrow L_\alpha$ (16)	439	0.097	$H\text{-}4_\beta \rightarrow L_\beta$ (44)	440	0.296	$H\text{-}3_\beta \rightarrow L_\beta$ (40)
S7	404	0.000[c]	$H\text{-}3_\alpha \rightarrow L_\alpha$ (26) $H\text{-}4_\beta \rightarrow L_\beta$ (23)	401	0.000[c]	$H\text{-}5_\beta \rightarrow L_\beta$ (34) $H\text{-}3_\alpha \rightarrow L_\alpha$ (22)	385	0.144	$H\text{-}1_\alpha \rightarrow L_\alpha$ (36) $H_\beta \rightarrow L{+}1_\beta$ (11)
S8	397	0.044	$H\text{-}1_\alpha \rightarrow L_\alpha$ (25) $H\text{-}6_\beta \rightarrow L_\beta$ (15)	396	0.099	$H\text{-}1_\alpha \rightarrow L_\alpha$ (35) $H_\beta \rightarrow L{+}1_\beta$ (14)	381	0.000[c]	$H\text{-}3_\alpha \rightarrow L_\alpha$ (29)
$\langle S^2 \rangle$	0.809(7.9%)			0.818(9.1%)			0.831(10.8%)		

[a] oscillator strengths for each transition; [b] main molecular orbital contribution for each transition; [c] all transitions with oscillator strengths smaller than 0.001 were assigned as 0

(*E*)-3-styrylquinoxalin-2(1*H*)-one, (**1a**).

^{1}H NMR (400 MHz, DMSO-d_6) δ 12.50 (s, 1H), 8.07 (d, J = 16.2 Hz, 1H), 7.78 (d, J = 8.2 Hz, 1H), 7.73 (d, J = 7.4 Hz, 2H), 7.63 (d, J = 16.2 Hz, 1H), 7.45 (m, 4H), 7.31 (d, J = 6.5 Hz, 2H).

^{13}C NMR (101 MHz, DMSO-d_6) δ 155.33, 153.45, 137.52, 136.45, 132.81, 132.15, 130.29, 129.84, 129.46, 128.81, 128.13, 123.97, 122.43, 115.73.

HRMS-ESI (+ mode) [M+H]: Calc = 249.1028; [M+H]: Exp 249.1023

(*E*)-3-styrylquinoxalin-2(1*H*)-one, (**1a**).

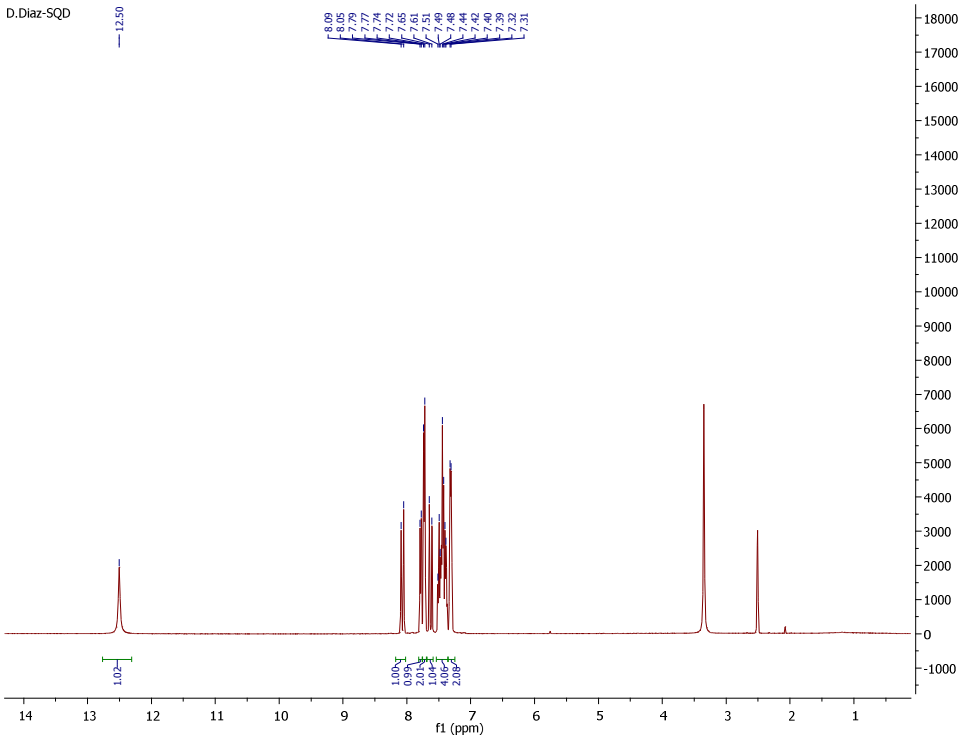

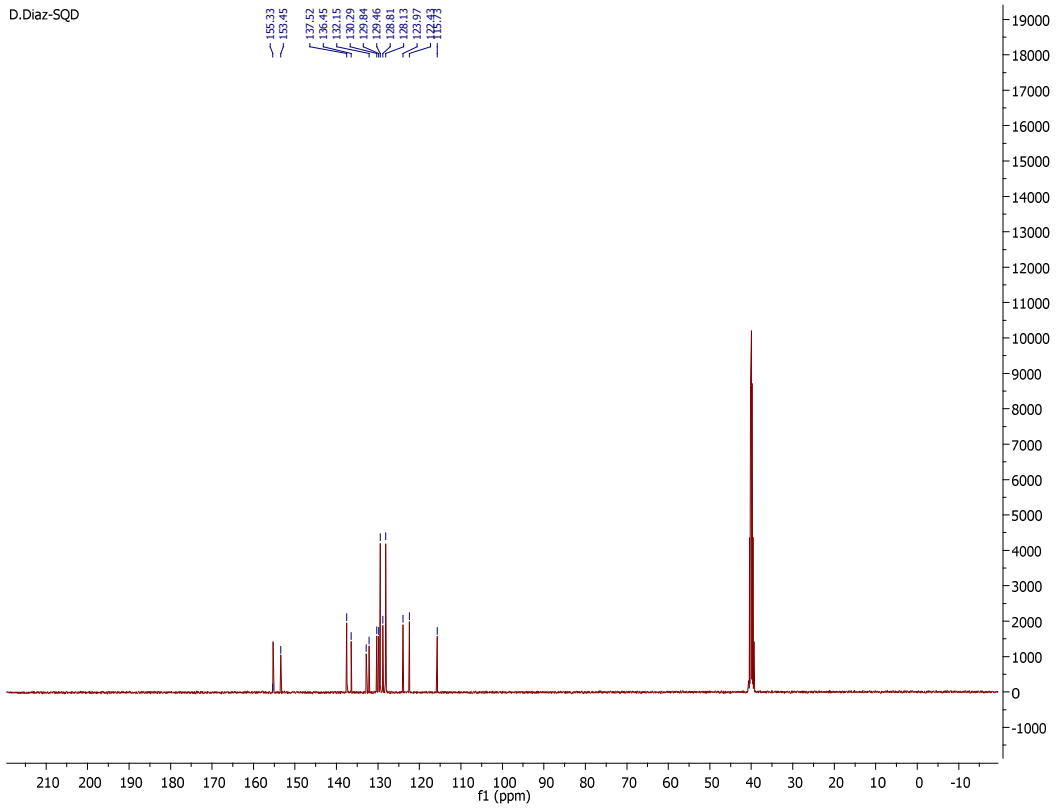
D.Diaz-SQD
155.33
153.45
137.52
136.45
132.15
130.29
129.84
129.46
128.81
128.13
123.97
112.93
f1 (ppm)

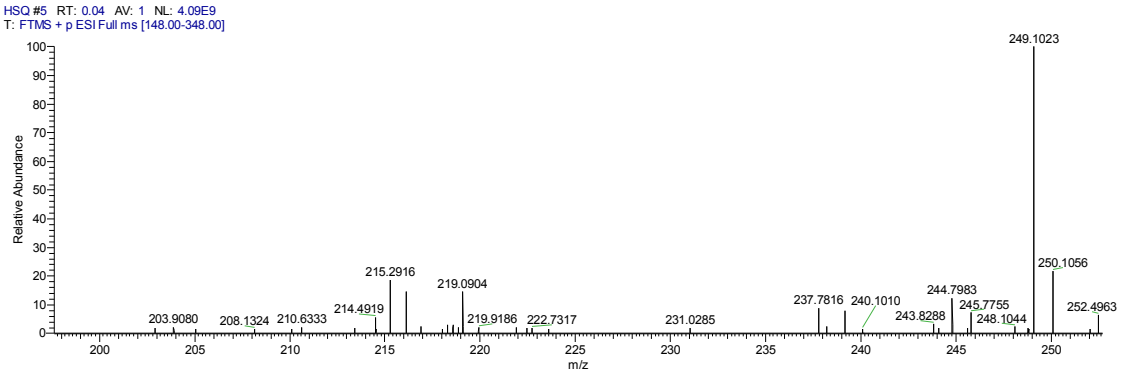
HSQ #5 RT: 0.04 AV: 1 NL: 4.09E9
T: FTMS + p ESI Full ms [148.00-348.00]
Relative Abundance
m/z
249.1023
250.1056
252.4963
215.2916
219.0904
214.4919
203.9080
208.1324
210.6333
219.9186
222.7317
231.0285
237.7816
240.1010
243.8288
244.7983
245.7755
248.1044

(*E*)-3-(4-methylstyryl)quinoxalin-2(1*H*)-one, (**1b**).

^{1}H NMR (400 MHz, DMSO-d_6) δ 12.47 (s, 1H), 8.02 (d, J = 16.2 Hz, 1H), 7.76 (d, J = 8.2 Hz, 1H), 7.58 (dd, J = 16.9, 12.1 Hz, 3H), 7.47 (t, J = 7.6 Hz, 1H), 7.32 – 7.26 (m, 2H), 7.23 (d, J = 7.7 Hz, 2H), 3.33 (s, 3H).

^{13}C NMR (50 MHz, DMSO-d_6) δ 154.74, 153.05, 139.14, 137.00, 133.21, 132.33, 131.56, 129.57, 128.22, 127.59, 123.42, 120.84, 115.18, 20.93.

HRMS-ESI (+ mode) [M+H]: Calc = 263.1184; [M+H]: Exp = 263.1179

(*E*)-3-(4-methylstyryl)quinoxalin-2(1*H*)-one, (**1b**).

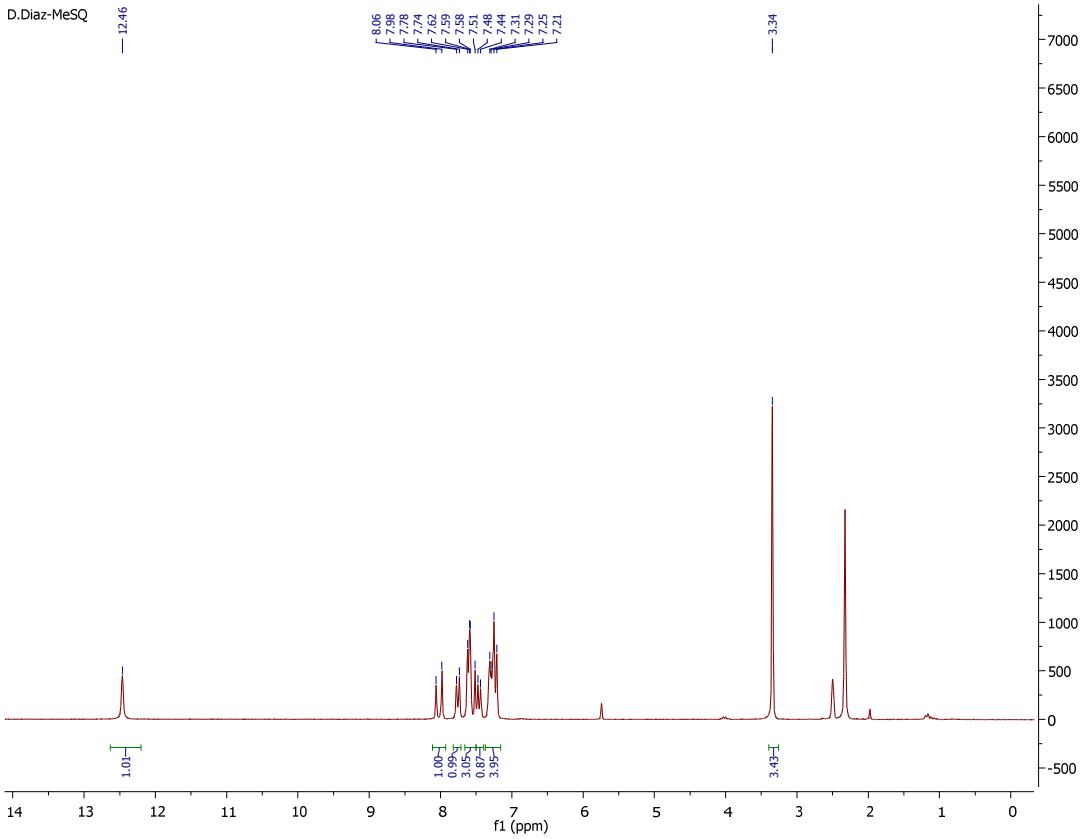

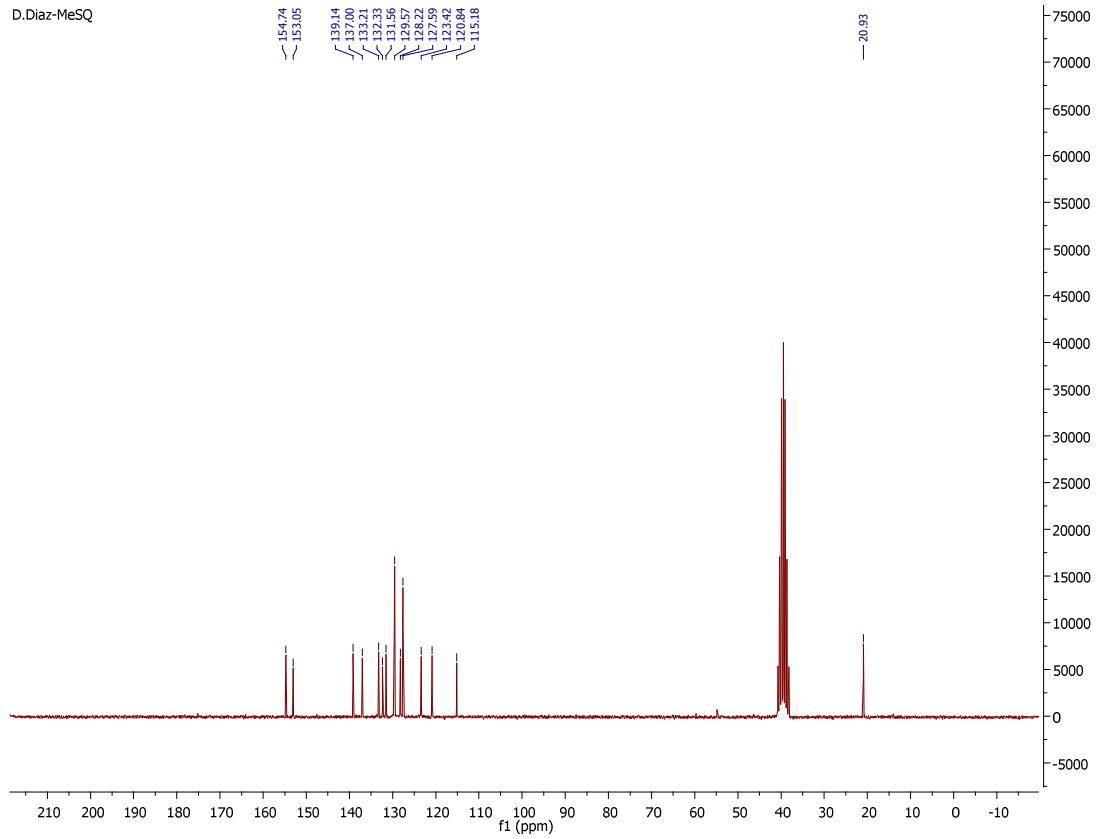
D.Diaz-MeSQ
154.74
153.05
139.14
137.00
133.21
132.33
131.56
129.57
128.22
127.59
123.42
120.84
115.18
20.93
f1 (ppm)

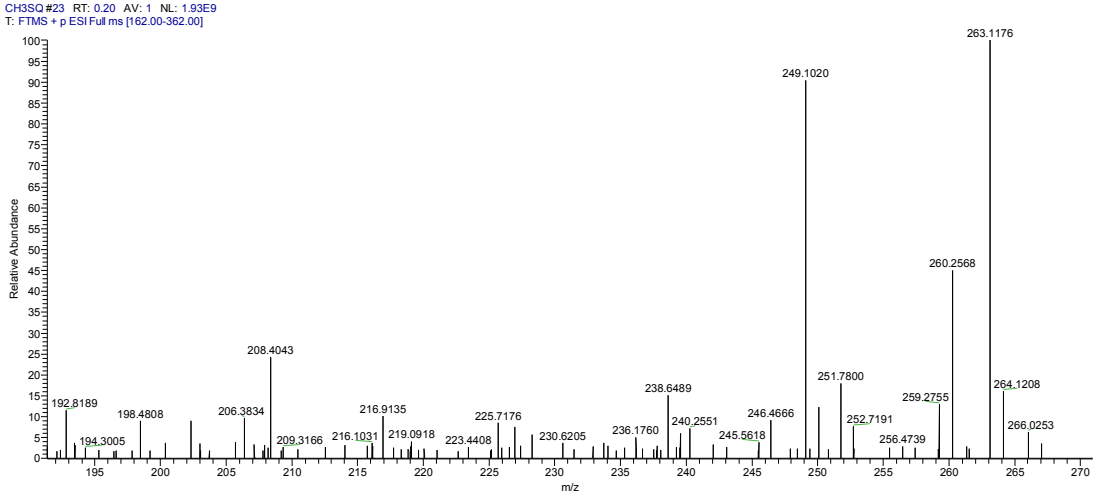
CH3SQ #23 RT: 0.20 AV: 1 NL: 1.93E9
T: FTMS + p ESI Full ms [162.00-362.00]
Relative Abundance
m/z
263.1176
249.1020
260.2568
208.4043
251.7800
264.1208
259.2755
238.6489
246.4666
252.7191
266.0253
240.2551
192.8189
198.4808
206.3834
216.9135
225.7176
194.3005
209.3166
216.1031
219.0918
223.4408
230.6205
236.1760
245.5618
256.4739

(*E*)-3-(4-methoxystyryl)quinoxalin-2(1*H*)-one, (**1c**).

^{1}H NMR (400 MHz, DMSO-d_6) δ 12.42 (d, J = 14.0 Hz, 1H), 8.02 (d, J = 16.2 Hz, 1H), 7.75 (d, J = 8.2 Hz, 1H), 7.68 (d, J = 8.2 Hz, 2H), 7.47 (dd, J = 16.0, 8.8 Hz, 2H), 7.31 – 7.26 (m, 2H), 6.99 (d, J = 8.2 Hz, 2H), 3.80 (s, 3H).

^{13}C NMR (101 MHz, DMSO-d_6) δ 160.72, 160.38, 154.81, 153.22, 136.88, 132.42, 131.51, 129.43, 129.31, 128.66, 128.14, 123.44, 119.45, 115.20, 114.49, 55.27.

HRMS-ESI (+ mode) [M+H]: Calc = 279.1134; [M+H]: Exp 279.1129

(*E*)-3-(4-methoxystyryl)quinoxalin-2(1*H*)-one, (**1c**).

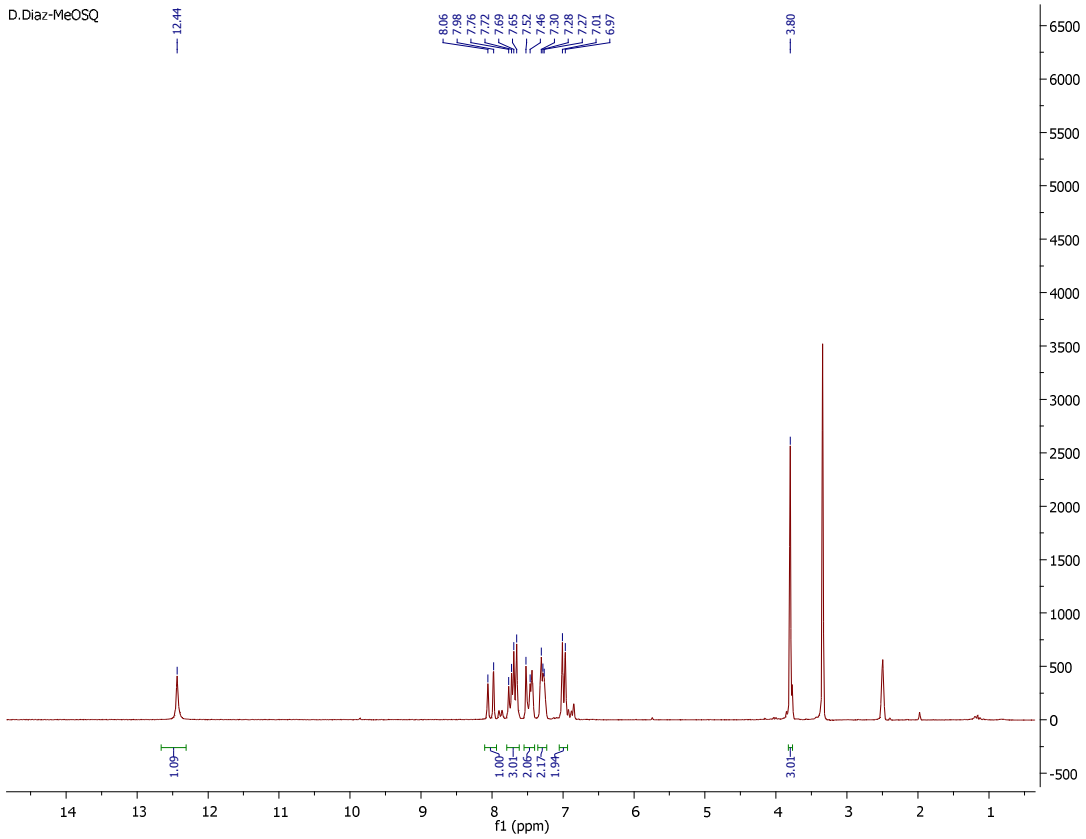

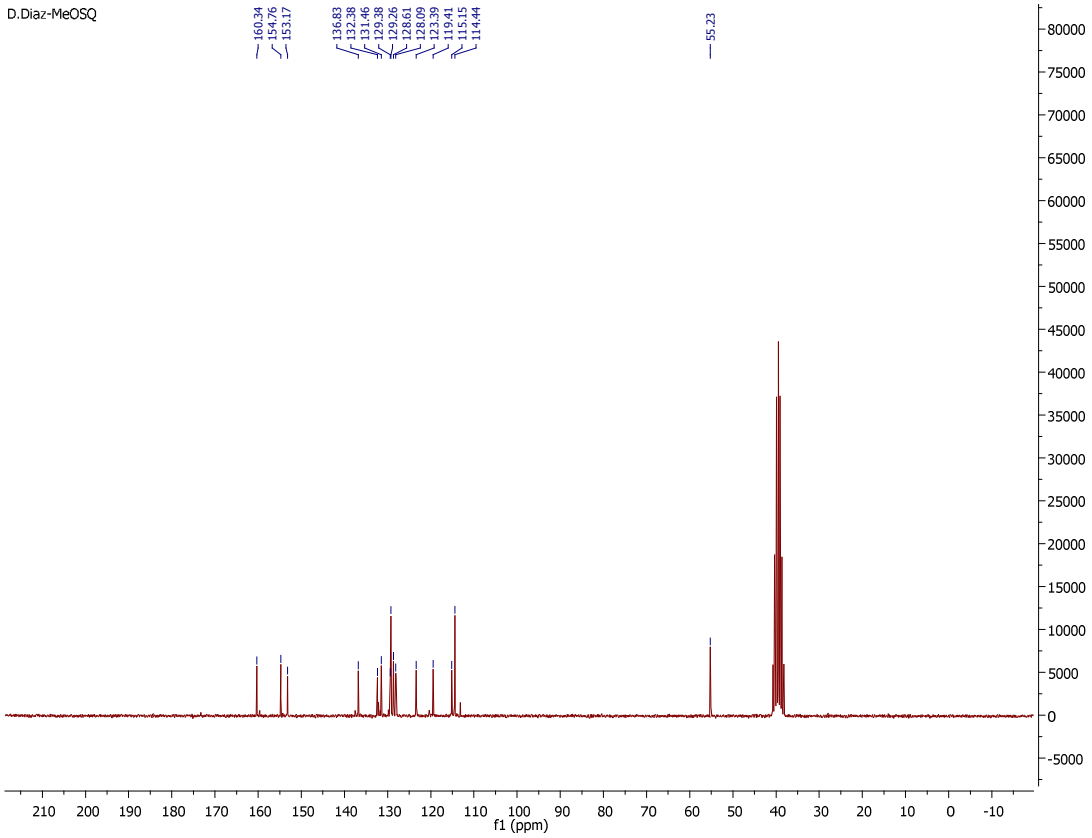
D.Diaz-MeOSQ
160.34
154.76
153.17
136.83
132.38
131.46
129.38
129.26
128.61
128.09
123.39
119.41
115.15
114.44
55.23
f1 (ppm)

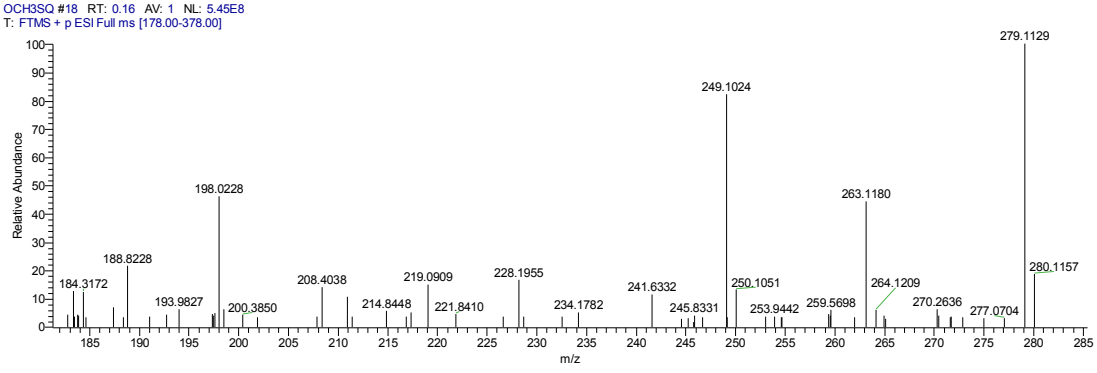
OCH3SQ #18 RT: 0.16 AV: 1 NL: 5.45E8
T: FTMS + p ESI Full ms [178.00-378.00]
Relative Abundance
m/z
279.1129
249.1024
198.0228
263.1180
188.8228
280.1157
184.3172
208.4038
219.0909
228.1955
241.6332
250.1051
264.1209
193.9827
200.3850
214.8448
221.8410
234.1782
245.8331
253.9442
259.5698
270.2636
277.0704

(*E*)-3-(4-(dimethylamino)styryl)quinoxalin-2(1*H*)-one, (**1d**).

^{1}H NMR (400 MHz, DMSO-d_6) δ 12.36 (s, 1H), 7.98 (d, J = 16.0 Hz, 1H), 7.72 (d, J = 8.0 Hz, 1H), 7.56 (d, J = 8.3 Hz, 2H), 7.41 (dd, J = 22.1, 12.0 Hz, 2H), 7.28 (t, J = 6.4 Hz, 2H), 6.75 (d, J = 8.3 Hz, 2H), 2.99 (s, 6H).

^{13}C NMR (101 MHz, DMSO-d_6) δ 155.36, 153.96, 151.61, 138.27, 133.08, 131.72, 129.70, 129.29, 128.30, 124.04, 123.85, 116.62, 115.56, 112.56, 40.22.

HRMS-ESI (+ mode) [M+H]: Calc = 292.1450; [M+H]: Exp 292.1431

(*E*)-3-(4-(dimethylamino)styryl)quinoxalin-2(1*H*)-one, (**1d**).

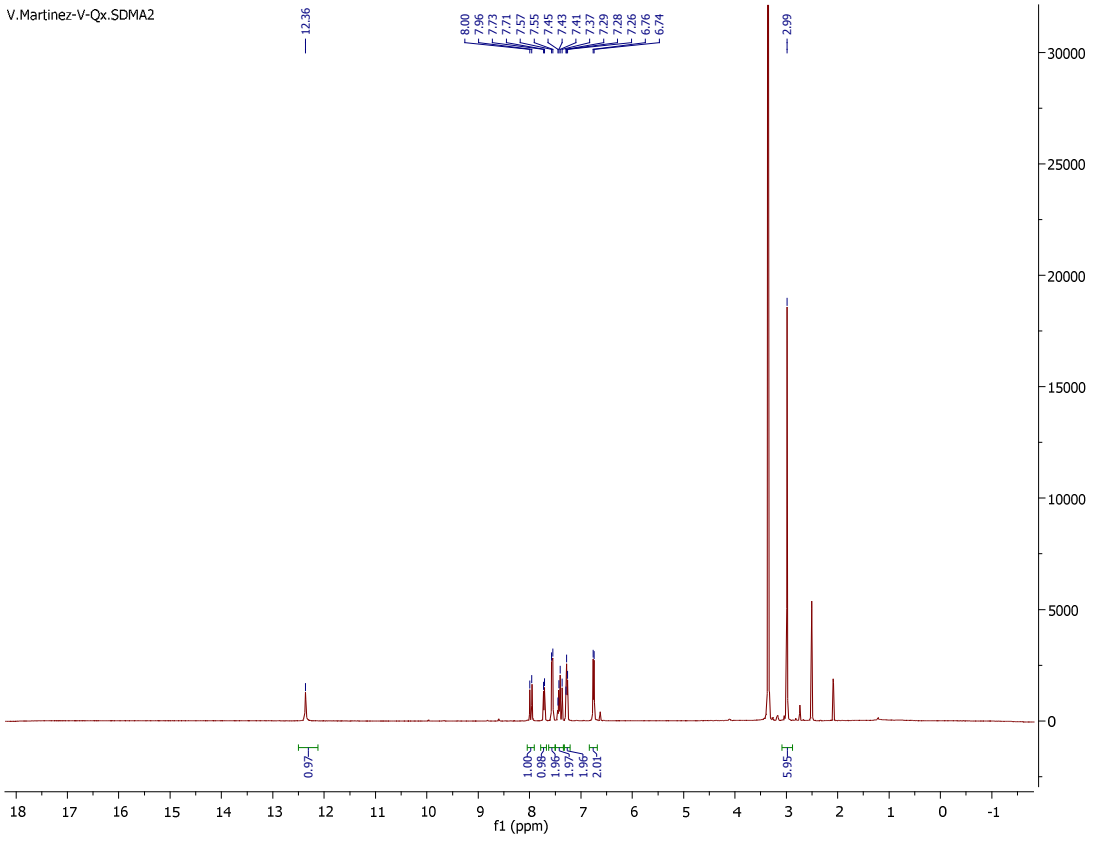

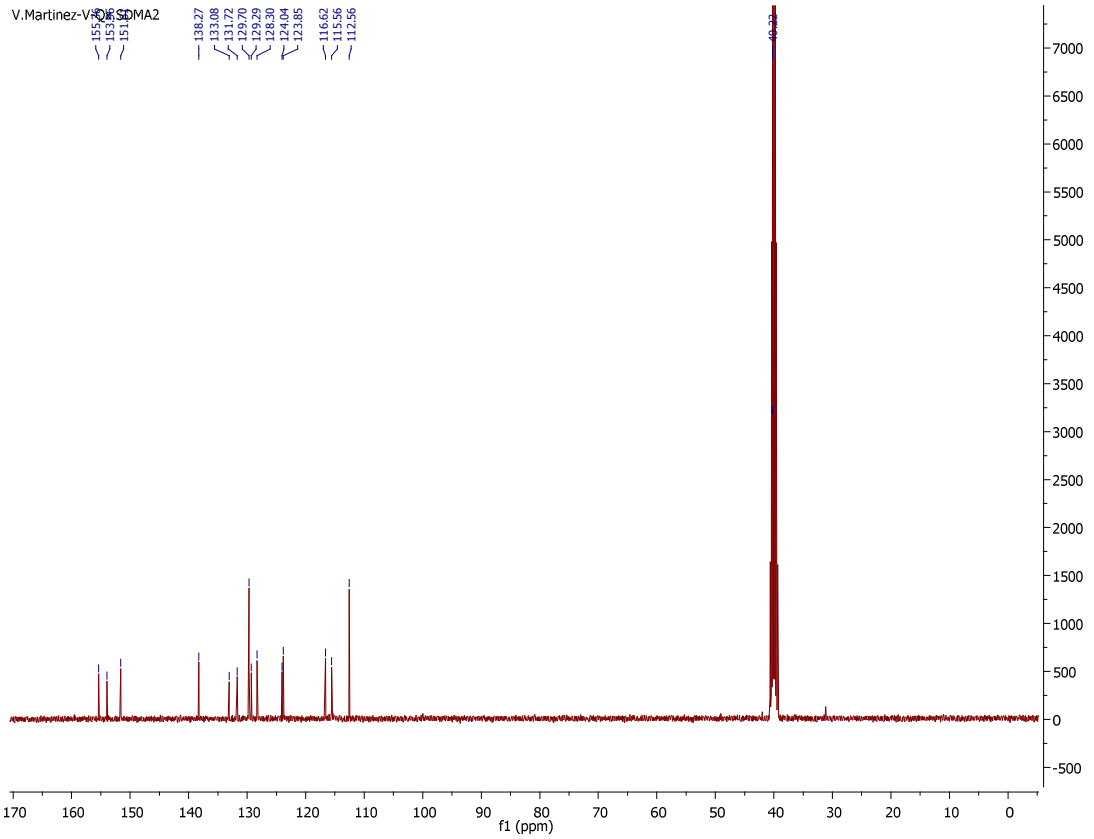
V.Martinez-Vazquez SDMA2
155.06
153.31
151.11
138.27
133.08
131.72
129.70
129.29
128.30
124.04
123.85
116.62
115.56
112.56
40.32
f1 (ppm)

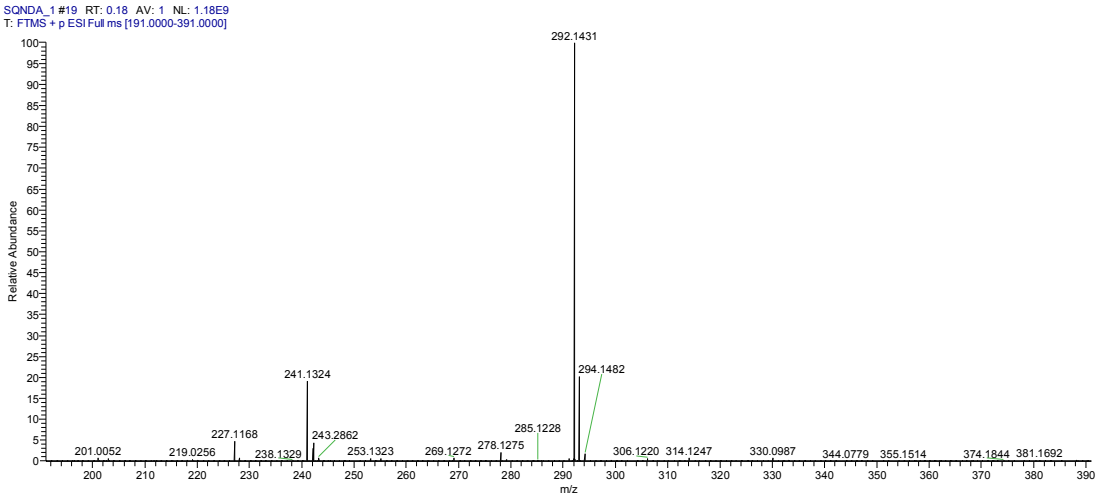
SQNDA_1 #19 RT: 0.18 AV: 1 NL: 1.18E9
T: FTMS + p ESI Full ms [191.0000-391.0000]
Relative Abundance
m/z
292.1431
294.1482
241.1324
227.1168
243.2862
285.1228
201.0052
219.0256
238.1329
253.1323
269.1272
278.1275
306.1220
314.1247
330.0987
344.0779
355.1514
374.1844
381.1692

3-{(*E*)-2-[4-(trifluoromethoxy)phenyl]vinyl}quinoxalin-2(1*H*)-one, (**1e**).

^{1}H NMR (400 MHz, DMSO-d_6) δ 12.52 (s, 1H), 8.07 (d, J = 16.2 Hz, 1H), 7.86 (d, J = 7.9 Hz, 2H), 7.77 (d, J = 8.1 Hz, 1H), 7.62 (d, J = 16.2 Hz, 1H), 7.49 (t, J = 7.6 Hz, 1H), 7.39 (d, J = 8.1 Hz, 2H), 7.30 (d, J = 7.4 Hz, 2H).

^{13}C NMR (101 MHz, DMSO-d_6) δ 154.76, 152.77, 148.69, 135.32, 132.30, 131.74, 130.01, 129.50, 128.41, 123.53, 123.23, 121.36, 118.78, 115.29.

HRMS-ESI (+ mode) [M+H]: Calc = 333.0851; [M+H]: Exp 333.0841

(*E*)-3-(4-(trifluoromethoxy)styryl)quinoxalin-2(1*H*)-one, (**1e**)

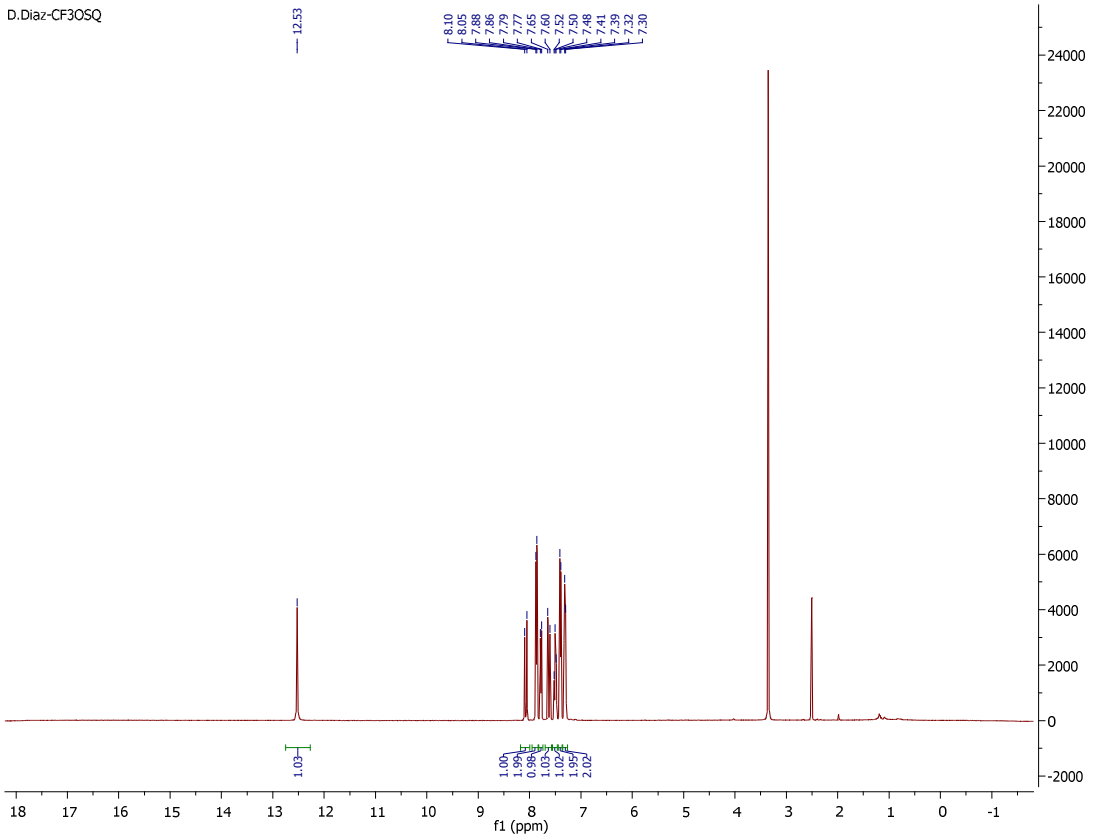

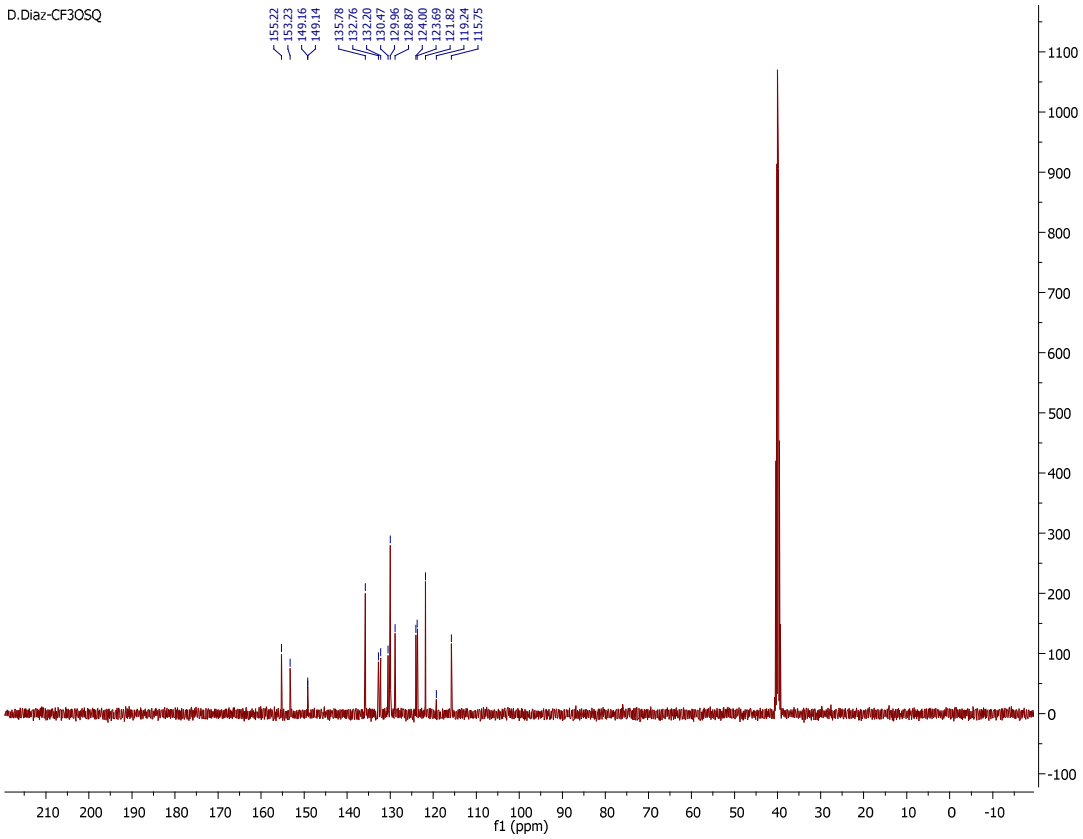
D.Diaz-CF3OSQ
155.22
153.23
149.16
149.14
135.78
132.76
132.20
130.47
129.96
128.87
124.00
123.69
121.82
119.24
115.75
f1 (ppm)

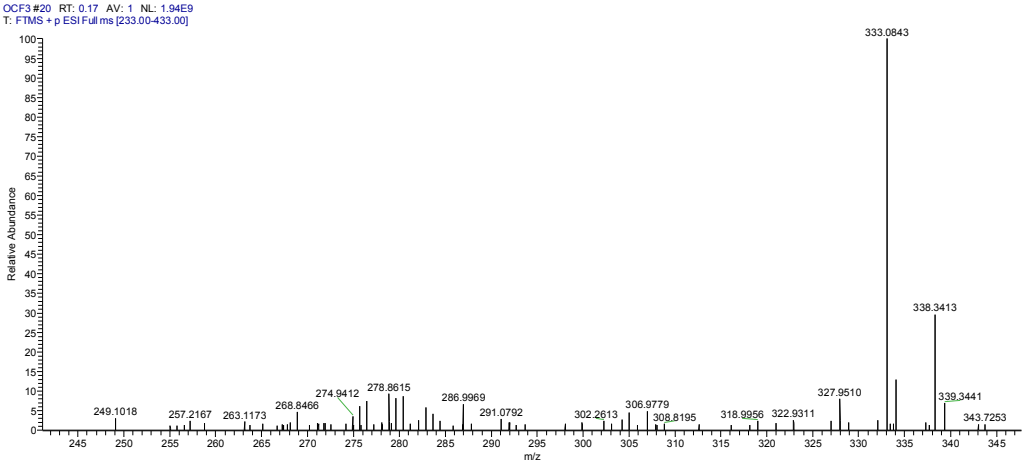
OCF3 #20 RT: 0.17 AV: 1 NL: 1.94E9
T: FTMS + p ESI Full ms [233.00-433.00]
Relative Abundance
m/z
333.0843
338.3413
339.3441
343.7253
327.9510
322.9311
318.9956
308.8195
306.9779
302.2613
291.0792
286.9969
278.8615
274.9412
268.8466
263.1173
257.2167
249.1018

(*E*)-3-(3,4-dimethoxystyryl)quinoxalin-2(1*H*)-one, (**1f**).

^{1}H NMR (400 MHz, DMSO-d_6) δ 12.47 (s, 1H), 8.04 (d, J = 16.2 Hz, 1H), 7.75 (d, J = 8.0 Hz, 1H), 7.49 (dd, J = 18.3, 11.9 Hz, 2H), 7.37 – 7.23 (m, 4H), 7.02 (d, J = 8.3 Hz, 1H), 3.86 (s, 3H), 3.81 (s, 3H).

^{13}C NMR (101 MHz, DMSO-d_6) δ 155.29, 153.70, 150.72, 149.54, 137.91, 132.92, 131.95, 129.91, 129.37, 128.58, 123.94, 122.32, 120.17, 115.66, 112.27, 110.36, 56.03, 56.01.

HRMS-ESI (+ mode) [M+H]: Calc = 309.1239; [M+H]: Exp 309.1230

(*E*)-3-(3,4-dimethoxystyryl)quinoxalin-2(1*H*)-one, (**1f**).

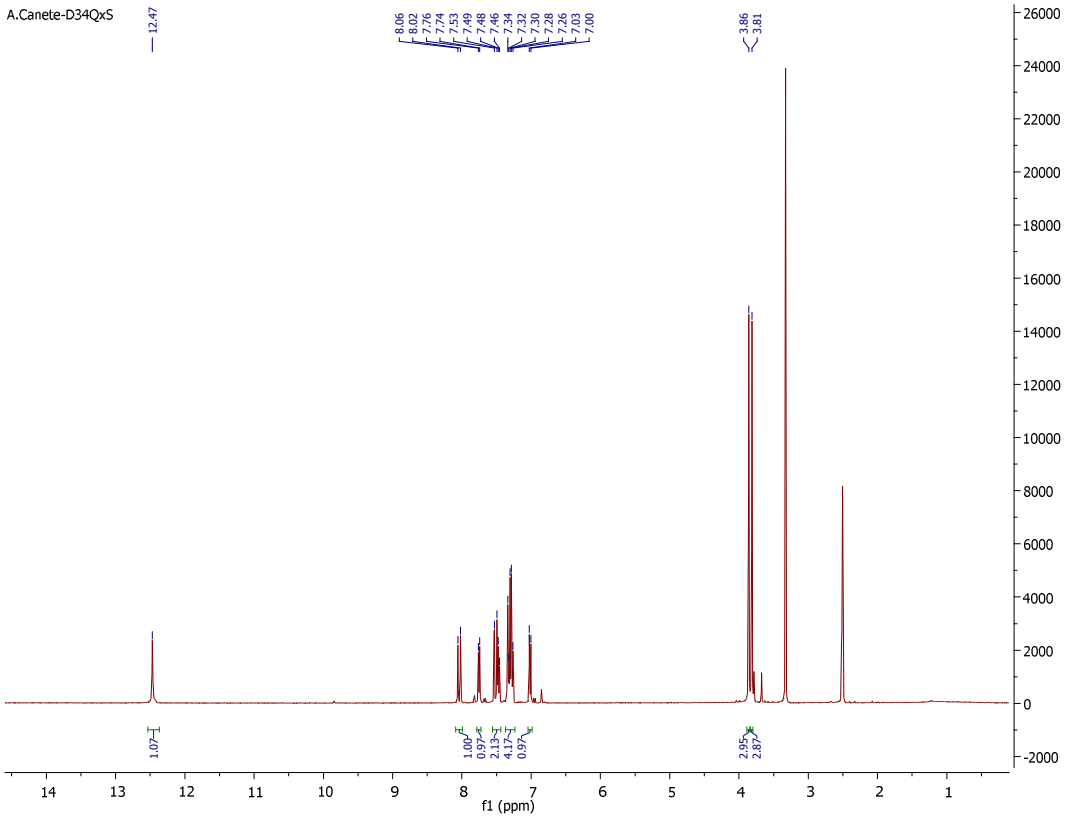

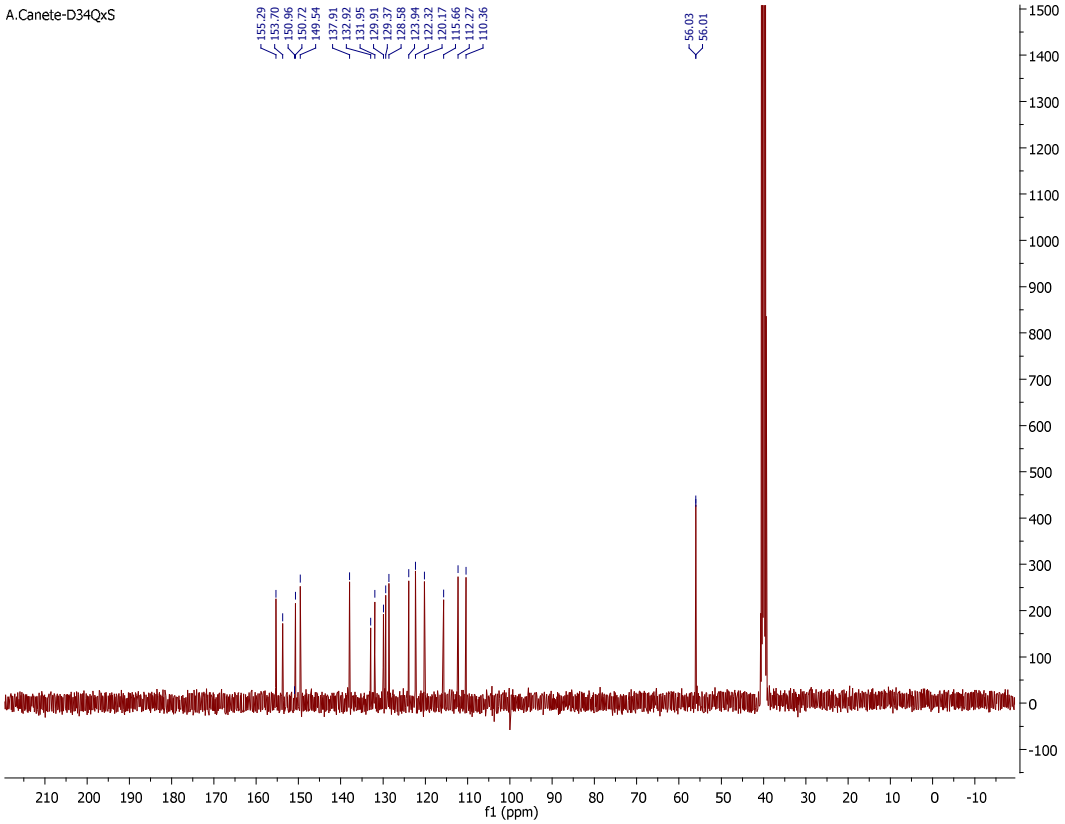
A.Canete-D34QxS
155.29
153.70
150.96
150.72
149.54
137.91
132.92
131.95
129.91
129.37
128.58
123.94
122.32
120.17
115.66
112.27
110.36
56.03
56.01
f1 (ppm)

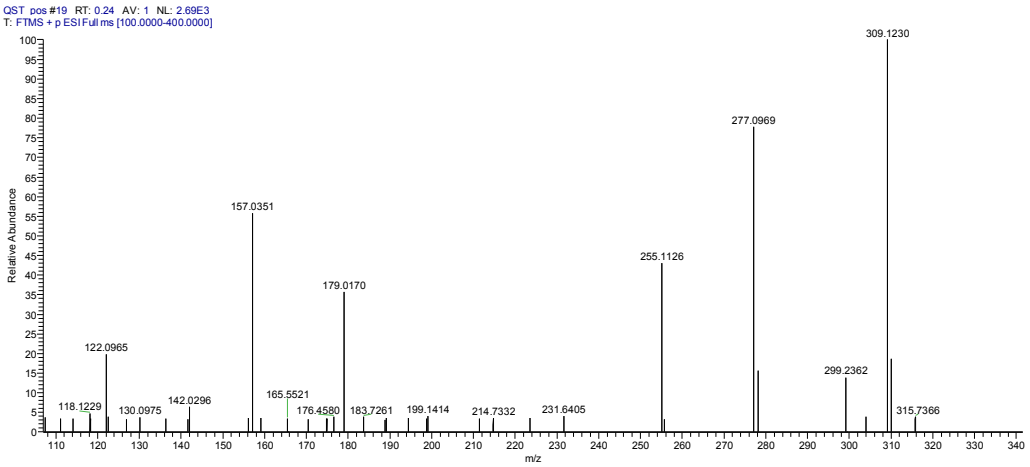
QST pos #19 RT: 0.24 AV: 1 NL: 2.69E3
T: FTMS + p ESI Full ms [100.0000-400.0000]
Relative Abundance
m/z
309.1230
277.0969
157.0351
255.1126
179.0170
122.0965
299.2362
315.7366
118.1229
130.0975
142.0296
165.5521
176.4580
183.7261
199.1414
214.7332
231.6405

(*E*)-3-(2,5-dimethoxystyryl)quinoxalin-2(1*H*)-one, (1g).

^{1}H NMR (400 MHz, DMSO-d_6) δ 12.47 (s, 1H), 8.32 (d, J = 16.4 Hz, 1H), 7.79 (dd, J = 8.3, 1.1 Hz, 1H), 7.64 (d, J = 16.4 Hz, 1H), 7.54 – 7.45 (m, 1H), 7.35 – 7.29 (m, 2H), 7.27 (d, J = 3.0 Hz, 1H), 7.04 (d, J = 9.0 Hz, 1H), 6.96 (dd, J = 9.0, 3.0 Hz, 1H), 3.86 (s, 3H), 3.79 (s, 3H).

^{13}C NMR (101 MHz, DMSO-d_6) δ 155.30, 153.78, 152.53, 132.86, 132.21, 132.12, 130.15, 128.79, 125.50, 123.95, 117.12, 115.71, 113.45, 112.01, 56.54, 55.98.

HRMS-ESI (+ mode) [M+H]: Calc = 309.1239; [M+H]: Exp 309.1229

(*E*)-3-(2,5-dimethoxystyryl)quinoxalin-2(1*H*)-one, (**1g**)

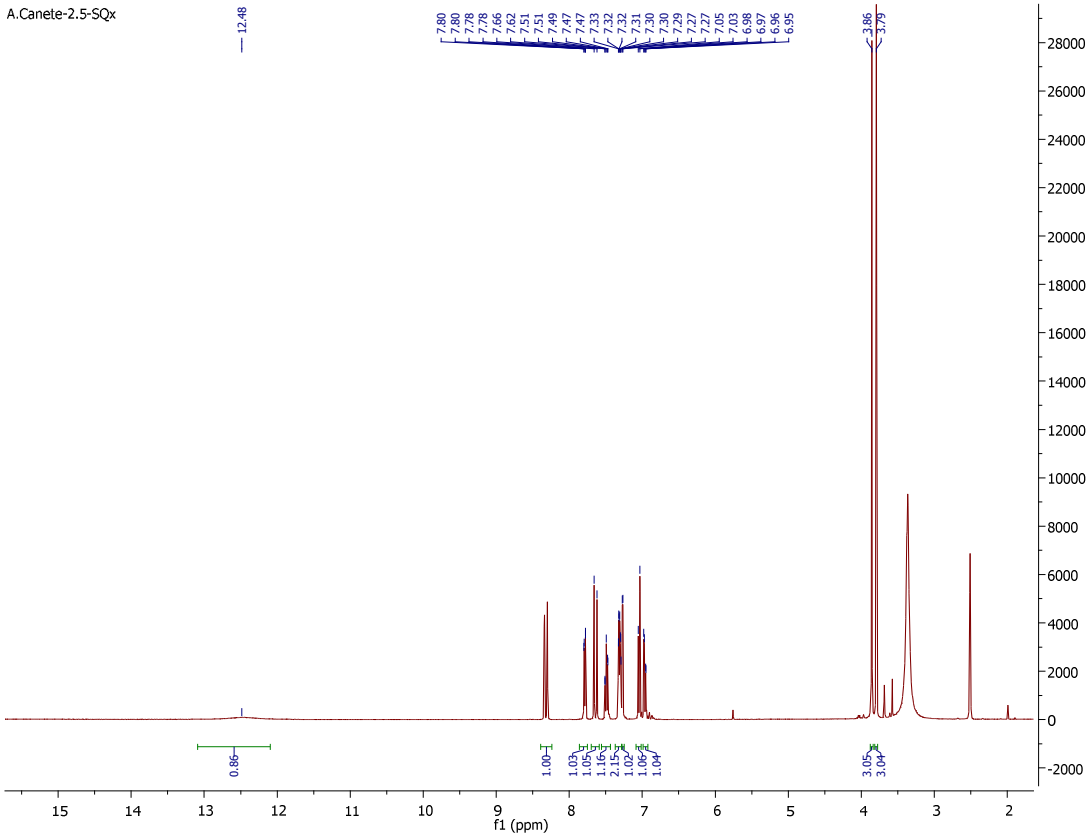

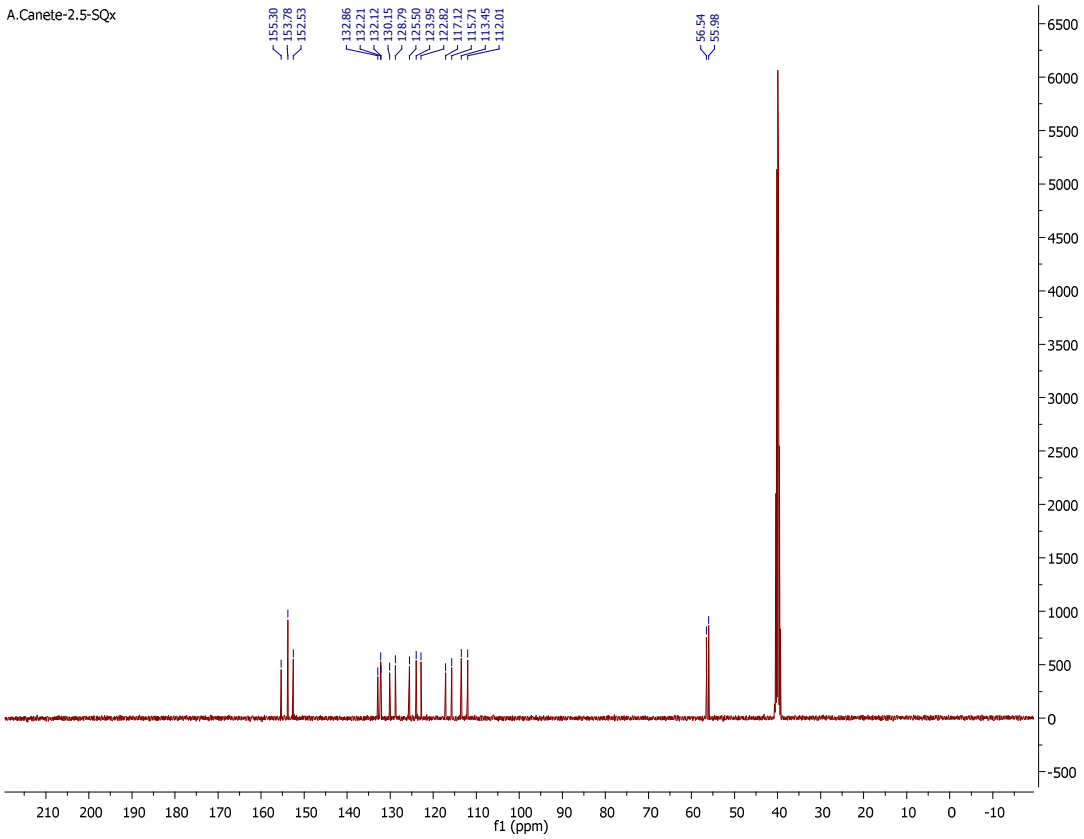
A.Canete-2.5-SQx
155.30
153.78
152.53
132.86
132.21
132.12
130.15
128.79
125.50
123.95
122.82
117.12
115.71
113.45
112.01
56.54
55.98
f1 (ppm)

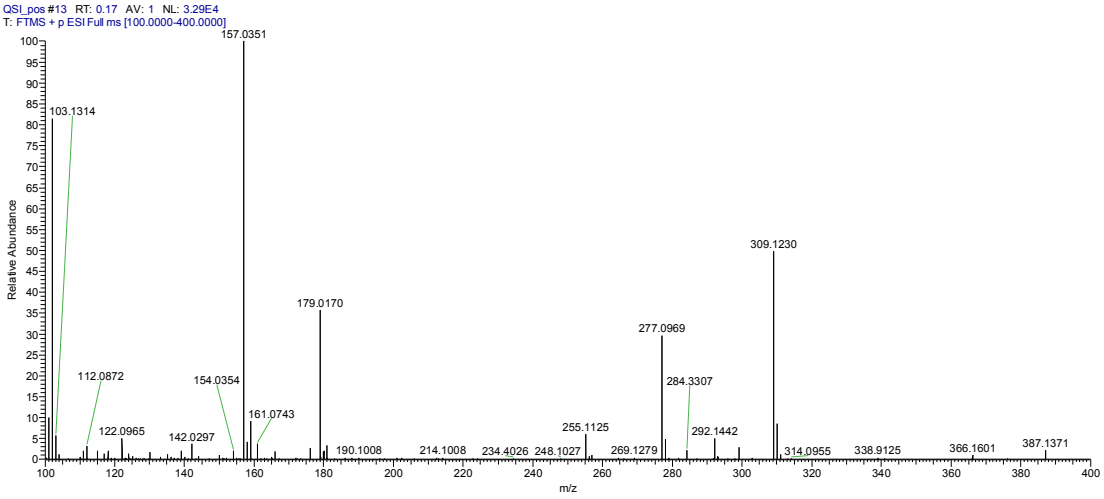
QSI_pos #13 RT: 0.17 AV: 1 NL: 3.29E4
T: FTMS + p ESI Full ms [100.0000-400.0000]
Relative Abundance
m/z
157.0351
103.1314
179.0170
309.1230
277.0969
112.0872
154.0354
284.3307
161.0743
255.1125
122.0965
292.1442
142.0297
190.1008
214.1008
234.4026
248.1027
269.1279
314.0955
338.9125
366.1601
387.1371